

# Signal reconstruction from noisy multichannel samples

Dong Cheng<sup>\*a,b</sup>, Xiaoxiao Hu<sup>†c</sup>, and Kit Ian Kou<sup>‡d</sup>

<sup>a</sup>Research Center for Mathematics and Mathematics Education, Beijing Normal University at Zhuhai, Zhuhai 519087, China

<sup>b</sup>Laboratory of Mathematics and Complex Systems (Ministry of Education), School of Mathematical Sciences, Beijing Normal University, Beijing 100875, China

<sup>c</sup>The First Affiliated Hospital of Wenzhou Medical University, Wenzhou Medical University, Wenzhou, Zhejiang, China

<sup>d</sup>Department of Mathematics, Faculty of Science and Technology, University of Macau, Macao, China

## Abstract

We consider the signal reconstruction problem under the case of the signals sampled in the multichannel way and with the presence of noise. Observing that if the samples are inexact, the rigorous enforcement of multichannel interpolation is inappropriate. Thus the reasonable smoothing and regularized corrections are indispensable. In this paper, we propose several alternative methods for the signal reconstruction from the noisy multichannel samples under different smoothing and regularization principles. We compare these signal reconstruction methods theoretically and experimentally in the various situations. To demonstrate the effectiveness of the proposed methods, the probability interpretation and the error analysis for these methods are provided. Additionally, the numerical simulations as well as some guidelines to use the methods are also presented.

**Keywords:** Signal reconstruction, multichannel samples, denoising, error analysis, smoothing, regularization.

**Mathematics Subject Classification (2010):** 39A12, 11R52, 41A05, 12E05.

## 1 Introduction

The main specialty of the multichannel sampling [1, 2] is that the samples are taken from multiple transformed versions of the function. The transformation can be the derivative, the Hilbert transform, or more general liner time invariant system [3]. The classical multichannel sampling theorem [1] is only available for the bandlimited functions in the sense of Fourier transform and

---

\*chengdong720@163.com

†huxiaoxiao@wmu.edu.cn

‡kikou@umac.mo

it has been generalized for the bandlimited functions in the sense of fractional Fourier transform (FrFT) [4], linear canonical transform (LCT) [5, 6] and offset LCT [7]. In a real application, only finitely many samples, albeit with large amount, are given in a bounded region [8]. That is, the underlying signal is time-limited. Thus, reconstruction by the sampling formulas for the bandlimited functions is inappropriate because the bandlimited functions cannot be time-limited by the uncertainty principle [9]. A time-limited function can be viewed as a period of a periodic function. Certain studies have been given to the sampling theorems for the periodic bandlimited functions [10, 11]. Moreover, the multichannel sampling approach has been extended to the time-limited functions [12].

Let  $\mathbb{T} := [0, 2\pi)$  be the unit circle and denote by  $L^p(\mathbb{T})$ ,  $1 \leq p < \infty$ , the totality of functions  $f(t)$  such that

$$\|f\|_p := \left( \frac{1}{2\pi} \int_{\mathbb{T}} |f(t)|^p dt \right)^{\frac{1}{p}} < \infty.$$

Let  $M \in \mathbb{Z}^+$ ,  $f, h_m \in L^2(\mathbb{T})$ , and define

$$g_m(t) = (f * h_m)(t) = \frac{1}{2\pi} \int_{\mathbb{T}} f(s) h_m(t - s) ds,$$

for  $1 \leq m \leq M$ . It was shown in [12] that there exist  $y_1(t), y_2(t), \dots, y_M(t)$  such that

$$\mathcal{T}_{\mathbf{N}} f(t) := \frac{1}{L} \sum_{m=1}^M \sum_{p=0}^{L-1} g_m\left(\frac{2\pi p}{L}\right) y_m\left(t - \frac{2\pi p}{L}\right) \quad (1.1)$$

satisfies the following interpolation consistency:

$$(\mathcal{T}_{\mathbf{N}} f * h_m)\left(\frac{2\pi p}{L}\right) = (f * h_m)\left(\frac{2\pi p}{L}\right), \quad 0 \leq p \leq L - 1, \quad 1 \leq m \leq M. \quad (1.2)$$

Here,  $g_m(t)$  is a filtered function with the input  $f(t)$  and the impulse response  $h_m(t)$ , and  $y_1(t), y_2(t), \dots, y_M(t)$  are determined by  $h_1(t), h_2(t), \dots, h_M(t)$ . The continuous function  $\mathcal{T}_{\mathbf{N}} f(t)$  is called a multichannel interpolation (MCI) for  $f$ . The MCI reveals that one can reconstruct a time-limited function  $f$  by using multiple types of samples simultaneously. If  $f$  is periodic bandlimited, it can be perfectly recovered by (1.1).

It is noted that to find a function satisfying the interpolation consistency (1.2) is to solve a system of  $N_s = LM$  equations. And the matrix involved in this inverse problem may have a large condition number if the sample sets  $\{g_m(\frac{2\pi p}{L}), 0 \leq p \leq L - 1\}, 1 \leq m \leq M$  have a high degree of relevance. In spite of this, in [8, 12], the authors showed that the large scale ( $N_s$ ) inverse problem could be converted to a simple inversion problem of small matrices ( $M \times M$ ) by partitioning the frequency band into small pieces. Moreover, the closed-form of the MCI formula as well as the FFT-based implementation algorithm (see Algorithm 1) were provided.

The MCI guarantees that a signal can be well reconstructed from its clean multichannel samples, little has been said about the case where the samples are noisy. It is of great significance to examine the errors that arise in the signal reconstruction by (1.1) in the presence of noise. In this paper, we consider the reconstruction problem under the situation that a signal  $f(t)$  is sampled in a multichannel way and the samples are corrupted by the additive noise, i.e., we will use the noisy samples

$$s_{m,p} = g_m\left(\frac{2\pi p}{L}\right) + \epsilon_{m,p}, \quad 0 \leq p \leq L - 1, \quad 1 \leq m \leq M, \quad (1.3)$$

to reconstruct  $f(t)$ . Here,  $\{\epsilon_{m,p}\}$  is an i.i.d. noise process with  $\mathbb{E}[\epsilon_{m,p}] = 0$ ,  $\text{Var}[\epsilon_{m,p}] = \sigma_\epsilon^2$ .

The interpolation of noisy data introduces the undesirable error in the reconstructed signal. There is a need to estimate the error of the MCI for the observations defined by (1.3). An accurate error estimate of the MCI in the presence of noise helps to design suitable reconstruction formulas from noisy multichannel samples. Note that the MCI applies to various kinds of sampling schemes, thus the error analysis can also be used to analyze what kinds of sampling schemes have a good performance in signal reconstruction in the noisy environment. In the current paper, we provide an error estimate for the MCI from noisy multichannel samples, and express the error as a function of the sampling rate as well as the parameters associated with sampling schemes. In addition, we will show how sampling rate and sampling schemes affect the reconstruction error caused by noise.

Based on the error estimate of the MCI in the noisy environment, we will provide a class of signal reconstruction methods by introducing some reasonable smoothing and regularized corrections to the MCI such that the reconstructed signal could be robust to noise. In other words, the reconstruction should not be affected much by small changes in the data. Besides, we need to make sure that the reconstructed signal will be convergent to the original signal as the sampling rate tends to infinity.

If  $f(t)$  is a periodic bandlimited signal, only the error caused by noise needs to be considered. Otherwise, the aliasing error should be taken into account as well. It is noted that the smoothing and regularization operations will restrain high frequency in general. It follows that to reduce the noise error by the methods based on smoothing or regularization may increase the aliasing error. Thus it is necessary to make a trade-off between the noise error and the aliasing error such that the reconstructed signal can be convergent to  $f$  in the non-bandlimited case as the sampling rate tends to infinity.

The objective of this paper is to study the aforementioned problems that arise in the signal reconstruction from noisy multichannel data. The main contributions are summarized as follows.

1. The error estimate of the signal reconstruction by the MCI from noisy samples is given.
2. We propose four methods, i.e., post-filtering, pre-filtering,  $l_1$  regularization and  $l_2$  regularization, to reduce the error caused by noise in the multichannel reconstruction. The parameters of post-filtering and pre-filtering are optimal in the sense of the expectation of mean square error (EMSE).
3. The convergence property of post-filtering is verified theoretically and experimentally. The numerical simulations as well as some guidelines to use the proposed signal reconstruction methods are also provided.

The rest of the paper is organized as follows. Section 2 briefly reviews the multichannel interpolation (MCI) and its FFT-based fast algorithm. The error estimate for the MCI of noisy samples is provided. In Section 3, the techniques of post-filtering, pre-filtering and regularized approximation are applied to reconstruct  $f$  from its noisy multichannel samples. The comparative experiments for the different methods are conducted in Section 4. Finally, conclusion and discussion are drawn at the end of the paper.

## 2 Error analysis of the MCI from noisy samples

### 2.1 The MCI and its fast implementation algorithm

We begin by reviewing the MCI in more detail. Let  $N_1, N_2 \in \mathbb{Z}$ , and  $I^{\mathbf{N}} = \{n : N_1 \leq n \leq N_2\}$ , we denote by  $B_{\mathbf{N}}$  the totality of the periodic bandlimited functions (trigonometric polynomials) with the following form:

$$f(t) = \sum_{n \in I^{\mathbf{N}}} a(n)e^{int}, \quad I^{\mathbf{N}} = \{n : N_1 \leq n \leq N_2\}.$$

The bandwidth of  $f$  is defined by the cardinality of  $I^{\mathbf{N}}$ , denoted by  $\mu(I^{\mathbf{N}})$ . The set  $I^{\mathbf{N}}$  can be expressed as  $I^{\mathbf{N}} = \bigcup_{j=1}^M I_j$ , where

$$I_j = \{n : N_1 + (j-1)L \leq n \leq N_1 + jL - 1\}.$$

We use the Fourier coefficients of  $h_m$  to define the  $M \times M$  matrix

$$\mathbf{H}_n = [b_m(n + jL - L)]_{jm}.$$

Suppose that  $\mathbf{H}_n$  is invertible for every  $n \in I_1$  and denote its inverse matrix as

$$\mathbf{H}_n^{-1} = \begin{bmatrix} q_{11}(n) & q_{12}(n) & \cdots & q_{1M}(n) \\ q_{21}(n) & q_{22}(n) & \cdots & q_{2M}(n) \\ \vdots & \vdots & & \vdots \\ q_{M1}(n) & q_{M2}(n) & \cdots & q_{MM}(n) \end{bmatrix}.$$

Then the interpolating function  $y_m$  in (1.1) is given by

$$y_m(t) = \sum_{n \in I^{\mathbf{N}}} r_m(n)e^{int}, \quad 1 \leq m \leq M,$$

where

$$r_m(n) = \begin{cases} q_{mj}(n + L - jL), & \text{if } n \in I_j, j = 1, 2, \dots, M, \\ 0 & \text{if } n \notin I^{\mathbf{N}}. \end{cases}$$

It was shown in [12] that if  $f$  is not bandlimited, the aliasing error of the MCI is given by

$$\sum_{n \notin I^{\mathbf{N}}} |a(n)|^2 + \sum_{k \notin \{1, 2, \dots, M\}} \sum_{n \in I_k} |a(n)|^2 \sum_{l=1}^M \left| \sum_{m=1}^M r_m(n + (l-k)L)b_m(n) \right|^2.$$

Moreover, the MCI can be implemented by a FFT-based algorithm (see Algorithm 1) and the well-known FFT interpolation [13] is a special case of the MCI.

### 2.2 The error estimate for the MCI of noisy samples

Given the noisy data (1.3), we define

$$f_{\mathbf{N}, \epsilon}(t) := \frac{1}{L} \sum_{m=1}^M \sum_{p=0}^{L-1} \left( g_m\left(\frac{2\pi p}{L}\right) + \epsilon_{m,p} \right) y_m\left(t - \frac{2\pi p}{L}\right).$$

---

**Algorithm 1:** FFT-based algorithm for MCI with complexity of  $\mathcal{O}(N_o \log N_o)$ .

---

**Input :**

1. The multichannel samples  $\mathbf{G} = [\mathbf{g}_1, \mathbf{g}_2, \dots, \mathbf{g}_M]$ , where  $\mathbf{g}_m$  is a vector consisting of  $L$  samples of  $g_m$ ;
2. The location of lower bound for the frequency band:  $N_1$ ;
3. The number of function values of  $\mathcal{T}_{\mathbf{N}}f(t)$ :  $N_o$ .

**Output:**

1. The vector  $\mathbf{f}_o$  consisting of  $N_o$  function values of  $\mathcal{T}_{\mathbf{N}}f(t)$ .
- 1 Multiply  $k$ -th row of  $\mathbf{G}$  by  $e^{\frac{-2\pi i N_1(k-1)}{L}}$ , obtain  $\mathbf{G}_e$ ;
  - 2 Take FFT of  $\mathbf{G}_e$  (for each column), obtain  $\tilde{\mathbf{G}}$ ;
  - 3 Compute  $\mathbf{A}_{L \times M}$ , where  $\mathbf{A}(k, :) = \tilde{\mathbf{G}}(k, :)\mathbf{H}_{N_1+k-1}^{-1}$ ;
  - 4 Flatten  $\mathbf{A}$  w.r.t. column, obtain  $\mathbf{a}$  ( $N_s$  length vector);
  - 5 Zero padding: add  $N_o - N_s$  zeros at the end of  $\mathbf{a}$ , obtain  $\mathbf{a}_z$ ;
  - 6 Compute IFFT for  $\mathbf{a}_z$ , obtain  $\mathbf{f}_e$ ;
  - 7 Multiply  $k$ -th element of  $\mathbf{f}_e$  by  $\frac{N_o}{L} e^{\frac{2\pi i N_1(k-1)}{N_o}}$ , obtain  $\mathbf{f}_o$ .
- 

If  $f \in B_{\mathbf{N}}$ , then

$$\begin{aligned}
& \mathbb{E} \left( \frac{1}{2\pi} \int_0^{2\pi} |f_{\mathbf{N},\epsilon}(t) - f(t)|^2 dt \right) \\
&= \mathbb{E} \left( \frac{1}{2\pi} \int_0^{2\pi} \left| \frac{1}{L} \sum_{m=1}^M \sum_{p=0}^{L-1} \epsilon_{m,p} y_m(t - \frac{2\pi p}{L}) \right|^2 dt \right) \\
&= \frac{1}{L^2} \mathbb{E} \sum_{m=1}^M \sum_{p=0}^{L-1} \sum_{m'=1}^M \sum_{p'=0}^{L-1} \epsilon_{m,p} \epsilon_{m',p'} \frac{1}{2\pi} \int_0^{2\pi} y_m(t - \frac{2\pi p}{L}) \overline{y_{m'}(t - \frac{2\pi p'}{L})} dt \\
&= \frac{1}{L^2} \sigma_{\epsilon}^2 \sum_{m=1}^M \sum_{p=0}^{L-1} \left( \frac{1}{2\pi} \int_0^{2\pi} |y_m(t - \frac{2\pi p}{L})|^2 dt \right) \\
&= \frac{\sigma_{\epsilon}^2}{L} \sum_{m=1}^M \|y_m\|_2^2 = \frac{\sigma_{\epsilon}^2}{L} \sum_{m=1}^M \sum_{n \in I^{\mathbf{N}}} |r_m(n)|^2.
\end{aligned}$$

Suppose that  $X, Y$  are independent random variables with the same normal distribution  $\mathcal{N}(0, \sigma^2)$ , it is easy to verify that  $\text{Var}(X^2) = 2\sigma^4$ ,  $\text{Var}(XY) = \sigma^4$ . Let

$$z(m, m', p, p') := \frac{1}{2\pi} \int_0^{2\pi} y_m(t - \frac{2\pi p}{L}) \overline{y_{m'}(t - \frac{2\pi p'}{L})} dt$$

From Hölder inequality, we have that

$$|z(m, m', p, p')|^2 \leq \|y_m\|_2^2 \|y_{m'}\|_2^2.$$

It follows that

$$\begin{aligned}
& \text{Var} \left( \frac{1}{2\pi} \int_0^{2\pi} |f_{\mathbf{N},\epsilon}(t) - f(t)|^2 dt \right) \\
&= \text{Var} \left( \frac{1}{2\pi} \int_0^{2\pi} \left| \frac{1}{L} \sum_{m=1}^M \sum_{p=0}^{L-1} \epsilon_{m,p} y_m \left( t - \frac{2\pi p}{L} \right) \right|^2 dt \right) \\
&\leq \frac{1}{L^4} \text{Var} \sum_{m=1}^M \sum_{p=0}^{L-1} \sum_{m'=1}^M \sum_{p'=0}^{L-1} \epsilon_{m,p} \epsilon_{m',p'} |z(m, m', p, p')| \\
&= \frac{1}{L^4} \sum_{m=1}^M \sum_{p=0}^{L-1} \sum_{m'=1}^M \sum_{p'=0}^{L-1} |z(m, m', p, p')|^2 \text{Var}(\epsilon_{m,p} \epsilon_{m',p'}) \\
&\leq \frac{2\sigma_\epsilon^4}{L^4} \sum_{m=1}^M \sum_{p=0}^{L-1} \sum_{m'=1}^M \sum_{p'=0}^{L-1} |z(m, m', p, p')|^2 \\
&\leq \frac{2\sigma_\epsilon^4}{L^2} \sum_{m=1}^M \sum_{m'=1}^M \|y_m\|_2^2 \|y_{m'}\|_2^2 \\
&= \frac{2\sigma_\epsilon^4}{L^2} \left( \sum_{m=1}^M \|y_m\|_2^2 \right)^2
\end{aligned}$$

Therefore the variance of mean square error is bounded and is not larger than twice the square of the expectation.

In order to show the mean square error of MCI caused by noise more clearly, we consider three concrete sampling schemes, namely, the reconstruction problem of  $f$  from (1) the samples of  $f$  (single-channel); (2) the samples of  $f$  and  $\mathcal{H}f$  (two-channel); (3) the samples of  $f$  and  $f'$  (two-channel). For simplicity, we abbreviate the MCI of the above types of samples as F1, FH2 and FD2 respectively and denote by  $N_s = LM$  the total number of samples. For F1, we have that  $M = 1$ ,  $N_s = LM = L$ . It easy to see that

$$r(n, \text{F1}, N_s) = 1 \quad \text{for} \quad -\frac{N_s}{2} + 1 \leq n \leq \frac{N_s}{2}.$$

For FH2, we have that  $M = 2$ ,  $N_s = 2L$ . Since

$$\mathbf{H}_n = \begin{bmatrix} 1 & -i \text{sgn}(n) \\ 1 & -i \text{sgn}(n+L) \end{bmatrix}.$$

It is clear that

$$\mathbf{H}_n^{-1} = \begin{bmatrix} \frac{1}{2} & \frac{1}{2} \\ -\frac{i}{2} & \frac{i}{2} \end{bmatrix} \quad \text{for} \quad -L+1 \leq n \leq -1, \quad \mathbf{H}_0^{-1} = \begin{bmatrix} 1 & 0 \\ -i & 1 \end{bmatrix}.$$

It follows that

$$r_1(n, \text{FH2}, N_s) = \begin{cases} \frac{1}{2}, & \text{if } 1 \leq |n| \leq L-1, \\ 0 & \text{if } n = L, \\ 1 & \text{if } n = 0. \end{cases}$$

$$r_2(n, \text{FH2}, N_s) = \begin{cases} -\frac{i}{2}, & \text{if } -L+1 \leq n \leq -1, \\ \frac{i}{2} & \text{if } 1 \leq n \leq L-1, \\ -i & \text{if } n = 0, \\ 1 & \text{if } n = L. \end{cases}$$

For FD2, by direct computations, we have that

$$\mathbf{H}_n = \begin{bmatrix} 1 & in \\ 1 & i(L+n) \end{bmatrix}, \quad \mathbf{H}_n^{-1} = \begin{bmatrix} \frac{L+n}{L} & -\frac{n}{L} \\ \frac{i}{L} & -\frac{i}{L} \end{bmatrix}.$$

It follows that

$$r_1(n, \text{FD2}, N_s) = \begin{cases} 1 + \frac{n}{L}, & \text{if } -L+1 \leq n \leq 0, \\ 1 - \frac{n}{L} & \text{if } 1 \leq n \leq L. \end{cases}$$

$$r_2(n, \text{FD2}, N_s) = \begin{cases} \frac{i}{L}, & \text{if } -L+1 \leq n \leq 0, \\ -\frac{i}{L} & \text{if } 1 \leq n \leq L. \end{cases}$$

To study FH2 and FD2, we assume that  $N_s$  is an even number and  $I^{\mathbf{N}} = \{n : -\frac{N_s}{2} + 1 \leq n \leq \frac{N_s}{2}\}$ . It should be noted that  $L = N_s$  for F1 because it is a single-channel interpolation. In contrast,  $L = \frac{N_s}{2}$  for FH2 and FD2 as they are two-channel interpolations. Thus, to compare the performance of the three interpolation methods under the same total number of samples  $N_s$ , one needs to keep in mind that  $L$  has different values for F1 and FH2.

Having introduced the Fourier coefficients of the interpolation functions for F1, FH2 and FD2, we have that

$$\frac{1}{N_s} \sum_{n \in I^{\mathbf{N}}} |r(n, \text{F1}, N_s)|^2 = 1,$$

$$\frac{1}{L} \sum_{m=1}^M \sum_{n \in I^{\mathbf{N}}} |r_m(n, \text{FH2}, N_s)|^2 = 1 + \frac{4}{N_s},$$

$$\frac{1}{L} \sum_{m=1}^M \sum_{n \in I^{\mathbf{N}}} |r_m(n, \text{FD2}, N_s)|^2 = \frac{2}{3} + \frac{28}{3N_s^2}.$$

Besides the theoretical error estimate, the experiments are conducted to compare the reconstructed results by F1, FH2 and FD2. Let

$$\phi(z) = \frac{0.08z^2 + 0.06z^{10}}{(1.3-z)(1.5-z)} + \frac{0.05z^3 + 0.09z^{10}}{(1.2+z)(1.3+z)}, \quad (2.1)$$

$$D(t, k_1, k_2) = \sum_{n=k_1}^{k_2} e^{int}, \quad (2.2)$$

$$\phi_B(t) = \phi(e^{it}) * D(t, -16, 16).$$

If  $k_2 = -k_1 > 0$ ,  $D(t, k_1, k_2)$  is the Dirichlet kernel of order  $k_2$ . We use  $\phi_B(t)$  as the test function. Obviously, it is bandlimited with the bandwidth 33. The theoretical errors, the experimental errors and the reconstructed results are shown in Figure 1 and some conclusions can be drawn as follows.

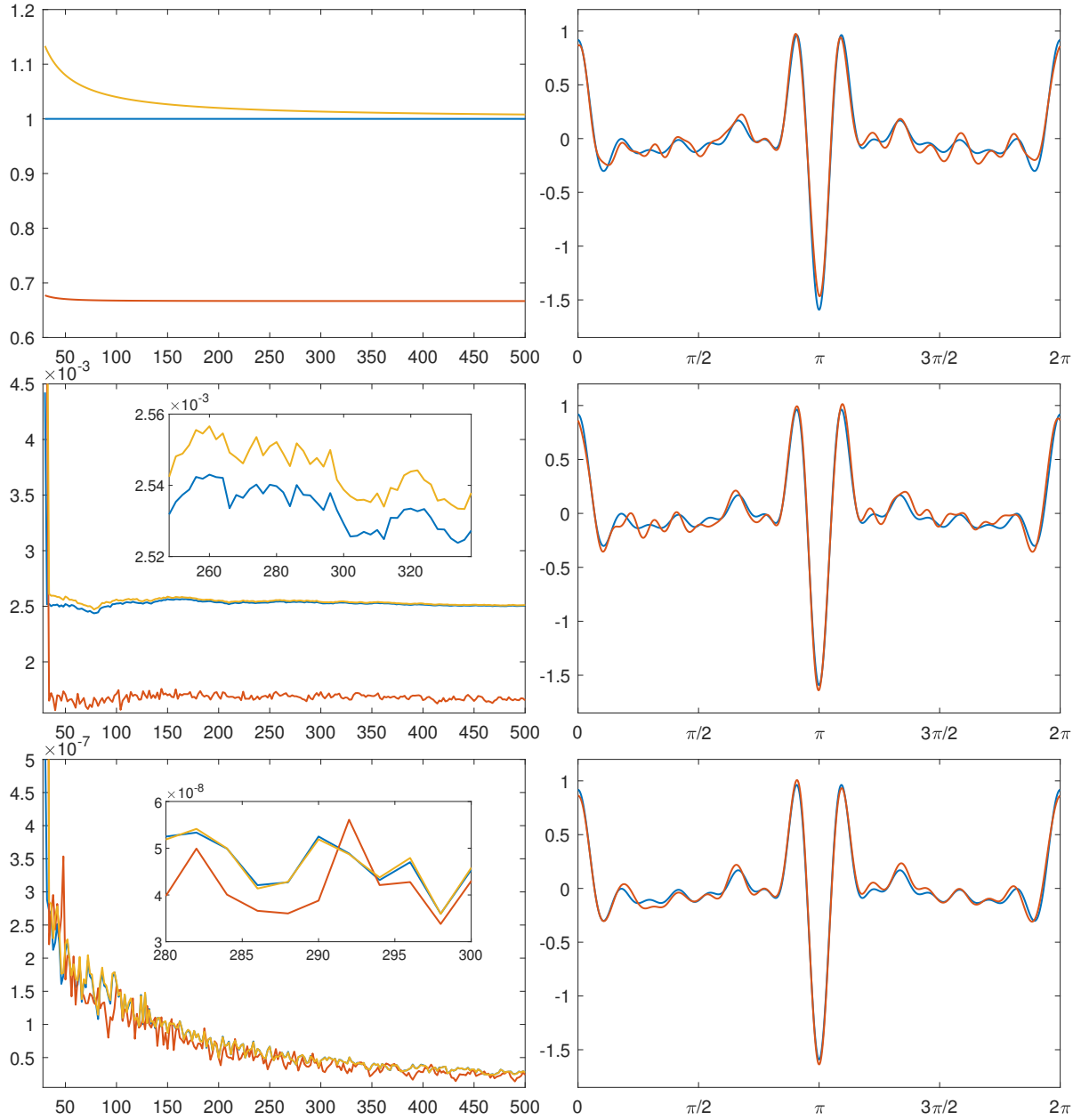


Figure 1: Left 1:  $\frac{1}{L} \sum_{m=1}^M \sum_{n \in I^N} |r_m(n)|^2$  for F1 (blue), FH2 (yellow) and FD2 (orange). Left 2: the average of the mean square error of 50 experiments for F1 (blue), FH2 (yellow) and FD2 (orange). Left 3: the variance of the mean square error of 50 experiments for F1 (blue), FH2 (yellow) and FD2 (orange). The horizontal axis in Left 1-3 represents the total number of samples, namely  $N_s$ . Right 1-3 are the reconstructed results (red lines) for F1, FH2 and FD2 respectively in the noisy environment with  $N_s = 56, \sigma_\epsilon = 0.05$ ; the blue line is the original test function  $\phi_B(t)$ .



1. FD2 performs better than F1 in terms of noise immunity and FH2 has the worst performance.
2. As the total number of samples increases, the expectation of mean square error (EMSE) would not decrease if there is no additional correction made in the multichannel reconstruction.
3. The variance of mean square error (VMSE) is bounded and it decreases as  $N_s$  increases.

**Remark 2.1** *In the second row first column of Figure 1, we see that the errors of F1, FH2 and FD2 become significantly large when  $N_s < 33$ . This is because the test function has the bandwidth 33, the reconstruction error is caused not only by noise but also by aliasing.*

### 3 Multichannel reconstruction from noisy samples

The MCI cannot work well if one observes noisy data because  $f_{\mathbf{N},\epsilon}(t)$  does not converge to  $f(t)$  in the sense of the expectation of mean square error (EMSE). To alleviate this problem, some smoothing corrections are required. If  $f(t)$  is bandlimited and the number of samples is larger than the bandwidth, we only need to consider the error caused by noise. Suppose that  $f \in B_{\mathbf{K}}, I^{\mathbf{K}} = \{k, K_1 \leq k \leq K_2\}$  and  $\mu(I^{\mathbf{K}}) \leq \mu(I^{\mathbf{N}}) = N_s$ , where  $N_s$  is the total number of samples. In this section, the techniques of post-filtering, pre-filtering, regularized approximation are applied to reconstruct  $f$  from noisy samples.

#### 3.1 Post-filtering

In [14], the ideal low-pass post-filtering is applied to the Shannon sampling formula and the error of signal reconstruction is also evaluated. Different from the previous work, we first derive the EMSE of the reconstruction by MCI and post-filtering. Then the filter is obtained by solving the optimization problem that minimizes the EMSE.

##### 3.1.1 Formulation of post-filtering

A natural smoothing approach for the reconstructed signal is to convolute  $f_{\mathbf{N},\epsilon}(t)$  with a function  $w(t) \in B_{\mathbf{K}}$ . Let

$$\tilde{f}(t, N_s, \mathbf{K}) = (f_{\mathbf{N},\epsilon} * w)(t).$$

Note that

$$f * D(\cdot, K_1, K_2)(t) = f(t)$$

provided that  $f \in B_{\mathbf{K}}$ . It follows that

$$\begin{aligned} & \tilde{f}(t, N_s, \mathbf{K}) - f(t) \\ &= f_{\mathbf{N},\epsilon} * w(t) - f * D(\cdot, K_1, K_2)(t) \\ &= [f * (w - D(\cdot, K_1, K_2))](t) + \frac{1}{L} \sum_{m=1}^M \sum_{p=0}^{L-1} \epsilon_{m,p} [y_m * w] \left(t - \frac{2\pi p}{L}\right). \end{aligned}$$

Since  $\{\epsilon_{m,p}\}$  is an i.i.d. noise process with  $\mathbb{E}[\epsilon_{m,p}] = 0$ , then

$$\begin{aligned} & \mathbb{E} \left( \left| \tilde{f}(t, N_s, \mathbf{K}) - f(t) \right|^2 \right) \\ &= \left| [f * (w - D(\cdot, K_1, K_2))] (t) \right|^2 + \frac{1}{L^2} \sum_{m=1}^M \sum_{p=0}^{L-1} \left| [y_m * w] \left( t - \frac{2\pi p}{L} \right) \right|^2 \mathbb{E}[\epsilon_{m,p}^2] \\ &= \left| [f * (w - D(\cdot, K_1, K_2))] (t) \right|^2 + \frac{1}{L^2} \sum_{m=1}^M \sum_{p=0}^{L-1} \left| [y_m * w] \left( t - \frac{2\pi p}{L} \right) \right|^2 \sigma_\epsilon^2. \end{aligned}$$

Denote the Fourier coefficient of  $w$  by  $\beta_k$ , it follows that

$$\begin{aligned} & \mathbb{E} \left( \frac{1}{2\pi} \int_0^{2\pi} \left| \tilde{f}(t, N_s, \mathbf{K}) - f(t) \right|^2 dt \right) \\ &= \frac{1}{2\pi} \int_0^{2\pi} \mathbb{E} \left| \tilde{f}(t, N_s, \mathbf{K}) - f(t) \right|^2 dt \\ &= \|f * (w - D(\cdot, K_1, K_2))\|_2^2 + \frac{\sigma_\epsilon^2}{L} \sum_{m=1}^M \|y_m * w\|_2^2 \\ &= \sum_{k=K_1}^{K_2} |a(k)(\beta_k - 1)|^2 + \frac{\sigma_\epsilon^2}{L} \sum_{m=1}^M \sum_{k=K_1}^{K_2} |r_m(k, \text{Type}, N_s) \beta_k|^2. \end{aligned}$$

**Remark 3.1** *Since the functions considered here are square integrable, the interchange of expectation and integral is permissible by the dominated convergence theorem. There are some similar cases happening elsewhere in the paper, we will omit the explanations.*

Let  $\boldsymbol{\beta} = (\beta_{K_1}, \dots, \beta_{K_2})^\top$  and

$$\Phi_1(\boldsymbol{\beta}) = \sum_{k=K_1}^{K_2} |a(k)(\beta_k - 1)|^2 + \frac{\sigma_\epsilon^2}{L} \sum_{m=1}^M \sum_{k=K_1}^{K_2} |r_m(k, \text{Type}, N_s) \beta_k|^2. \quad (3.1)$$

Since  $||\beta_k| - 1| \leq |\beta_k - 1|$  and the equality holds only if  $\beta_k \geq 0$ , it follows that

$$\Phi_1(\boldsymbol{\beta}_+) - \Phi_1(\boldsymbol{\beta}) = \sum_{k=K_1}^{K_2} |a(k)| (||\beta_k| - 1| - |\beta_k - 1|) \leq 0,$$

where  $\boldsymbol{\beta}_+ = (|\beta_{K_1}|, \dots, |\beta_{K_2}|)^\top$ . Thus, if

$$\boldsymbol{\beta}^* = (\beta_{K_1}^*, \dots, \beta_{K_2}^*)^\top = \arg \min_{\boldsymbol{\beta}} \Phi_1(\boldsymbol{\beta}),$$

then  $\beta_k^* \geq 0$  for every  $K_1 \leq k \leq K_2$ . To minimize  $\Phi_1(\boldsymbol{\beta})$ , we rewrite it as follows:

$$\Phi_1(\boldsymbol{\beta}) = \|\mathbf{A}_+ \boldsymbol{\beta} - \mathbf{a}_+\|_2^2 + \frac{\sigma_\epsilon^2}{L} \sum_{m=1}^M \|\mathbf{R}_{m,+} \boldsymbol{\beta}\|_2^2,$$

where

$$\mathbf{a}_+ = (|a(K_1)|, \dots, |a(K_2)|)^T, \quad \mathbf{A}_+ = \text{diag}(\mathbf{a}_+),$$

$$\mathbf{R}_{m,+} = \text{diag}(|r_m(K_1, \text{Type}, N_s)|, \dots, |r_m(K_2, \text{Type}, N_s)|).$$

Differentiating  $\Phi_1(\boldsymbol{\beta})$  with respect to  $\boldsymbol{\beta}$  and solving  $\nabla\Phi_1(\boldsymbol{\beta}) = 0$ , we obtain the optimal solution for minimizing the expectation of mean square error. That is,

$$\boldsymbol{\beta}^* = \left( \mathbf{A}_+^T \mathbf{A}_+ + \frac{\sigma_\epsilon^2}{L} \sum_{m=1}^M \mathbf{R}_{m,+}^T \mathbf{R}_{m,+} \right)^{-1} \mathbf{A}_+^T \mathbf{a}_+. \quad (3.2)$$

### 3.1.2 Estimation of spectral density

The formula (3.2) gives the optimal values for the parameters of post-filtering, to minimize the difference (EMSE) between the filtered and the original (clean) signal  $f(t)$ . The key problem is that the square of absolute value of  $a(n)$ , namely the spectral density of  $f(t)$ , is unknown in typical cases. Thus we have to estimate the value of  $|a(n)|^2$  from the noisy multichannel samples.

There are various techniques for spectral density estimation. The representative methods are periodogram, Welch's method, autoregressive model and moving-average model, etc. Here, we provide an unbiased estimation for  $|a(n)|^2$  by using the uncorrelatedness of signal and noise.

Let

$$\mathbf{s}_m = (s_{m,0}, s_{m,1}, \dots, s_{m,L-1})^T, \quad 1 \leq m \leq M,$$

$$\mathbf{g}_m = (g_m(t_0), g_m(t_1), \dots, g_m(t_{L-1}))^T, \quad t_p = \frac{2\pi p}{L}, 1 \leq m \leq M,$$

$$\boldsymbol{\epsilon}_m = (\epsilon_{m,0}, \epsilon_{m,1}, \dots, \epsilon_{m,L-1})^T, \quad 1 \leq m \leq M,$$

then

$$\mathbf{s}_m = \mathbf{g}_m + \boldsymbol{\epsilon}_m.$$

To estimate  $|a(n)|^2$ , we need to introduce the vector  $\mathbf{d}_0$  and  $\mathbf{d}_\epsilon$ , where

$$\mathbf{d}_0 = \frac{1}{L} \begin{bmatrix} \mathbf{F}_L \mathbf{U}_L \mathbf{g}_1 \\ \mathbf{F}_L \mathbf{U}_L \mathbf{g}_2 \\ \vdots \\ \mathbf{F}_L \mathbf{U}_L \mathbf{g}_M \end{bmatrix}, \quad \mathbf{d}_\epsilon = \frac{1}{L} \begin{bmatrix} \mathbf{F}_L \mathbf{U}_L \mathbf{s}_1 \\ \mathbf{F}_L \mathbf{U}_L \mathbf{s}_2 \\ \vdots \\ \mathbf{F}_L \mathbf{U}_L \mathbf{s}_M \end{bmatrix}. \quad (3.3)$$

Here,  $\mathbf{F}_L$  is the  $L$ -th order DFT matrix

$$\mathbf{F}_L = \begin{bmatrix} \omega^0 & \omega^0 & \omega^0 & \dots & \omega^0 \\ \omega^0 & \omega^1 & \omega^2 & \dots & \omega^{L-1} \\ \omega^0 & \omega^2 & \omega^4 & \dots & \omega^{2(L-1)} \\ \vdots & \vdots & \vdots & \ddots & \vdots \\ \omega^0 & \omega^{L-1} & \omega^{2(L-1)} & \dots & \omega^{(L-1)^2} \end{bmatrix} \quad (3.4)$$

with  $\omega = e^{-2\pi i/L}$  and  $\mathbf{U}_L$  is a diagonal matrix

$$\mathbf{U}_L = \begin{bmatrix} \omega^0 & & & & \\ & \omega^{N_1} & & & \\ & & \mathbf{0} & & \\ & & & \omega^{2N_1} & \\ \mathbf{0} & & & & \ddots \\ & & & & & \omega^{(L-1)N_1} \end{bmatrix}. \quad (3.5)$$

Note that  $\mathbf{F}_L^* = L\mathbf{F}_L^{-1}$ ,  $\mathbf{U}_L^* = \mathbf{U}_L^{-1}$  and  $\{\epsilon_{m,p}\}$  is an i.i.d. noise process, it follows that

$$\mathbb{E}[\mathbf{d}_\epsilon \mathbf{d}_\epsilon^*] = \frac{\sigma_\epsilon^2}{L} \mathbf{I} + \mathbf{d}_0 \mathbf{d}_0^*.$$

Let  $\mathbf{B}$  be a  $N_s$  by  $N_s$  matrix and the entry in the  $m$ -th row and  $n$ -th column of  $\mathbf{B}$  is

$$\mathbf{B}(m, n) = \begin{cases} \mathbf{H}_{N_1+k-1}^{-1}(j+1, i+1), & \text{if } m = iL + k, n = jL + k, \\ 0 & \text{otherwise,} \end{cases}$$

where  $1 \leq k \leq L$  and  $0 \leq i, j \leq M-1$ . By direct computations, we have that

$$\mathbb{E}[\mathbf{B} \mathbf{d}_\epsilon \mathbf{d}_\epsilon^* \mathbf{B}^*] = \mathbf{B} \left( \frac{\sigma_\epsilon^2}{L} \mathbf{I} + \mathbf{d}_0 \mathbf{d}_0^* \right) \mathbf{B}^* = \frac{\sigma_\epsilon^2}{L} \mathbf{B} \mathbf{B}^* + \mathbf{B} \mathbf{d}_0 \mathbf{d}_0^* \mathbf{B}^*.$$

If  $f$  is bandlimited, it can be verified that the diagonal element of  $\mathbf{B} \mathbf{d}_0 \mathbf{d}_0^* \mathbf{B}^*$  is equal to  $|a(n)|^2$  (by a similar method for proving Lemma 1 in [12]). It follows that the diagonal element of

$$\mathbf{B} \mathbf{d}_\epsilon \mathbf{d}_\epsilon^* \mathbf{B}^* - \frac{\sigma_\epsilon^2}{L} \mathbf{B} \mathbf{B}^* \quad (3.6)$$

is an unbiased estimation for  $|a(n)|^2$ .

To validate the effectiveness of the above method for estimating spectral density, the noisy multichannel samples are applied to estimate  $|a(n)|^2$  by the formula (3.6) experimentally. We will perform a series of experiments under different quantities and types of samples. Let

$$f(t) = \sum_{n=N_1}^{N_2} a(n) e^{int}, \quad N_1 = -2, N_2 = 3 \quad (3.7)$$

be the test function, where  $a(-2) = 1 + i$ ,  $a(-1) = 2 - i$ ,  $a(0) = 1$ ,  $a(1) = 2 + i$ ,  $a(2) = 1 - i$ ,  $a(3) = 0$ . The mean square error (MSE) for estimating the spectral density of  $f$  is defined by

$$\delta_{sde} = \frac{\sum_{n=N_1}^{N_2} \left| |a(n)|^2 - \tilde{A}(n) \right|^2}{N_2 - N_1 + 1},$$

where  $\tilde{A}(n)$  is the  $(N_1 - n + 1)$ -th diagonal element of  $\mathbf{B} \mathbf{d}_\epsilon \mathbf{d}_\epsilon^* \mathbf{B}^* - \frac{\sigma_\epsilon^2}{L} \mathbf{B} \mathbf{B}^*$ . To show the performance of the estimation more accurately, each experiment will be repeated 1000 times and the corresponding average MSE is an approximation of the expectation of MSE.

Table 1: The experimental results of multichannel based method for spectral density estimation. The first row displays the total number of samples used in each experiment. The second and third rows display the number of samples of  $f$  and  $f'$  used in each experiment respectively. The error of spectral density estimation is given in the last row.

$N_s$	6	6	30	60	60	300	600	600
$f$	6	3	30	60	30	300	600	300
$f'$	0	3	0	0	30	0	0	300
Average MSE	0.3390	0.3427	0.0673	0.0335	0.0356	0.0071	0.0034	0.0036

The experimental results are presented in Table 1. The second column indicates that if we use 6 samples of  $f$  to estimate spectral density, the expectation of MSE is approximately equal to 0.3390. It can be seen that the expectation of MSE for spectral density estimation varies in inverse proportion to the total number of samples. In other words, the experimentally obtained MSE, i.e.  $\delta_{sde}$ , tends to 0 as the total number of samples goes to infinity and if the same total number of samples are used to estimate spectral density, the fluctuations of MSE caused by different sampling schemes are not significant. Besides, it is noted that the traditional single-channel based method for spectral density estimation can not utilize the multichannel information to improve the accuracy. By contrast, the proposed multichannel based method fuses the different types of samples, thereby extending the scope of application and enhancing the precision, as seen from the column four and six of Table 1.

### 3.2 Pre-filtering

If  $f$  is bandlimited, it can be expressed as

$$f(t) = \frac{1}{L} \sum_{m=1}^M \mathbf{g}_m^T \mathbf{U}_L \mathbf{F}_L \mathbf{v}_m(t),$$

where

$$\mathbf{v}_m(t) = (v_{m,N_1}(t), v_{m,N_1+1}(t), \dots, v_{m,L+N_1-1}(t))^T, \quad v_{m,n}(t) = \sum_{k=1}^M q_{mk}(n) e^{i(n+kL-L)t}$$

for  $n \in I_1$ . We consider to filter the noisy multichannel samples  $\mathbf{s}_1, \mathbf{s}_2, \dots, \mathbf{s}_M$  by modifying the frequency components in the DFT domain. Let

$$\tilde{\mathbf{s}}_m = \mathbf{U}_L^{-1} \mathbf{F}_L^{-1} \mathbf{\Lambda}_m \mathbf{F}_L \mathbf{U}_L \mathbf{s}_m, \quad \mathbf{\Lambda}_m = \text{diag}(\lambda_{m,N_1}, \lambda_{m,N_1+1}, \dots, \lambda_{m,L+N_1-1}),$$

and construct a function of form

$$\check{f}(t) = \frac{1}{L} \sum_{m=1}^M \tilde{\mathbf{s}}_m^T \mathbf{U}_L \mathbf{F}_L \mathbf{v}_m(t) = \frac{1}{L} \sum_{m=1}^M \mathbf{s}_m^T \mathbf{U}_L \mathbf{F}_L \mathbf{\Lambda}_m \mathbf{v}_m(t).$$

In this part, we want to determine the values of  $\lambda_{m,n}$ ,  $1 \leq m \leq M, n \in I_1$ , such that  $\check{f}(t)$  be

a good estimation of  $f(t)$ . The square of absolute value for the difference of  $f(t)$  and  $\check{f}(t)$  is

$$\begin{aligned} \left| \check{f}(t) - f(t) \right|^2 &= \left| \frac{1}{L} \sum_{m=1}^M (\mathbf{g}_m^T + \boldsymbol{\epsilon}_m^T) \mathbf{U}_L \mathbf{F}_L \boldsymbol{\Lambda}_m \mathbf{v}_m(t) - \frac{1}{L} \sum_{m=1}^M \mathbf{g}_m^T \mathbf{U}_L \mathbf{F}_L \mathbf{v}_m(t) \right|^2 \\ &= \left| \frac{1}{L} \sum_{m=1}^M \mathbf{g}_m^T \mathbf{U}_L \mathbf{F}_L (\boldsymbol{\Lambda}_m - \mathbf{I}) \mathbf{v}_m(t) + \frac{1}{L} \sum_{m=1}^M \boldsymbol{\epsilon}_m^T \mathbf{U}_L \mathbf{F}_L \mathbf{v}_m(t) \right|^2. \end{aligned}$$

**Remark 3.2** To blend the information of different types of samples, the frequency band has to be partitioned (shown as follows for the case of  $M = 3, L = 5$ ). The vector  $\mathbf{v}_m(t)$  plays an important role in the multichannel reconstruction. The frequency bands of the  $L$  elements for  $\mathbf{v}_m(t)$  are located in the  $L$  positions corresponding to different colors. The role of  $\mathbf{U}_L$  is to shift the zero-frequency component to the center of spectrum.



Let

$$\begin{aligned} u_1(t) &= \frac{1}{L} \sum_{m=1}^M \mathbf{g}_m^T \mathbf{U}_L \mathbf{F}_L (\boldsymbol{\Lambda}_m - \mathbf{I}) \mathbf{v}_m(t), \\ u_2(t) &= \frac{1}{L} \sum_{m=1}^M \boldsymbol{\epsilon}_m^T \mathbf{U}_L \mathbf{F}_L \boldsymbol{\Lambda}_m \mathbf{v}_m(t). \end{aligned}$$

We have that

$$\begin{aligned} \mathbb{E} (|u_2(t)|^2) &= \mathbb{E} \left( \frac{1}{L^2} \sum_{m=1}^M |\boldsymbol{\epsilon}_m^T \mathbf{U}_L \mathbf{F}_L \boldsymbol{\Lambda}_m \mathbf{v}_m(t)|^2 \right) \\ &= \mathbb{E} \left( \frac{1}{L^2} \sum_{m=1}^M |\boldsymbol{\epsilon}_m^T \mathbf{z}_m(t)|^2 \right) \\ &= \mathbb{E} \left( \frac{1}{L^2} \sum_{m=1}^M \sum_{p \in I_1} \sum_{k \in I_1} \epsilon_{m,p-N_1+1} \overline{\epsilon_{m,k-N_1+1}} z_{m,p}(t) \overline{z_{m,k}(t)} \right) \\ &= \frac{\sigma_\epsilon^2}{L^2} \sum_{m=1}^M \sum_{p \in I_1} |z_{m,p}(t)|^2. \end{aligned}$$

Here, we denote  $\mathbf{U}_L \mathbf{F}_L \boldsymbol{\Lambda}_m \mathbf{v}_m(t)$  by

$$\mathbf{z}_m(t) = (z_{m,N_1}(t), z_{m,N_1+1}(t), \dots, z_{m,L+N_1-1}(t))^T$$

and the first equality and last equality are direct consequences of the independence of noise. By the definition of  $r_m(n)$ , we know that  $q_{mk}(n) = r_m(n + kL - L)$  for  $n \in I_1$ , it follows that

$$v_{m,n}(t) = \sum_{k=1}^M r_m(n + kL - L) e^{i(n+kL-L)t}, \quad n \in I_1.$$

Thus

$$\begin{aligned} z_{m,p}(t) &= \omega^{(p-N_1)N_1} \sum_{n \in I_1} \lambda_{m,n} v_{m,n}(t) \omega^{(n-N_1)(p-N_1)} \\ &= \sum_{k=1}^M \sum_{n \in I_1} \omega^{n(p-N_1)} \lambda_{m,n} r_m(n+kL-L) e^{i(n+kL-L)t}. \end{aligned}$$

It follows from the Parseval's identity that

$$\begin{aligned} \mathbb{E} \left( \frac{1}{2\pi} \int_0^{2\pi} |u_2(t)|^2 dt \right) &= \frac{1}{2\pi} \int_0^{2\pi} \mathbb{E} (|u_2(t)|^2) dt \\ &= \frac{\sigma_\epsilon^2}{L^2} \sum_{m=1}^M \sum_{p \in I_1} \frac{1}{2\pi} \int_0^{2\pi} |z_{m,p}(t)|^2 dt \\ &= \frac{\sigma_\epsilon^2}{L^2} \sum_{m=1}^M \sum_{p \in I_1} \sum_{k=1}^M \sum_{n \in I_1} |\lambda_{m,n} r_m(n+kL-L)|^2 \\ &= \frac{\sigma_\epsilon^2}{L} \sum_{m=1}^M \sum_{k=1}^M \sum_{n \in I_1} |\lambda_{m,n} r_m(n+kL-L)|^2. \end{aligned}$$

By direct computations, we have that

$$\begin{aligned} u_1(t) &= \sum_{m=1}^M \sum_{n \in I_1} (\lambda_{m,n} - 1) d_m(n) v_{m,n}(t), \\ &= \sum_{m=1}^M \sum_{n \in I_1} \sum_{k=1}^M (\lambda_{m,n} - 1) d_m(n) r_m(n+kL-L) e^{i(n+kL-L)t} \end{aligned}$$

where

$$d_m(n) = \sum_{k=1}^M a(n+kL-L) b_m(n+kL-L).$$

It follows from the Parseval's identity that

$$\frac{1}{2\pi} \int_0^{2\pi} |u_1(t)|^2 dt = \sum_{k=1}^M \sum_{n \in I_1} \left| \sum_{m=1}^M (\lambda_{m,n} - 1) d_m(n) r_m(n+kL-L) \right|^2.$$

Note that  $|\check{f}(t) - f(t)|^2 = |u_1(t) + u_2(t)|^2$  and by the independence of noise, we can use the integrations of  $u_1$  and  $u_2$  to express the expectation of MSE; that is,

$$\begin{aligned} &\mathbb{E} \left( \frac{1}{2\pi} \int_0^{2\pi} |\check{f}(t) - f(t)|^2 dt \right) \\ &= \mathbb{E} \left( \frac{1}{2\pi} \int_0^{2\pi} |u_1(t) + u_2(t)|^2 dt \right) \\ &= \frac{1}{2\pi} \int_0^{2\pi} |u_1(t)|^2 dt + \mathbb{E} \left( \frac{1}{2\pi} \int_0^{2\pi} |u_2(t)|^2 dt \right). \end{aligned}$$

It follows that

$$\begin{aligned} & \mathbb{E} \left( \frac{1}{2\pi} \int_0^{2\pi} |\check{f}(t) - f(t)|^2 dt \right) \\ &= \sum_{k=1}^M \left\| \sum_{m=1}^M \tilde{\mathbf{R}}_{m,k} \mathbf{D}_m \boldsymbol{\lambda}_m - \tilde{\mathbf{R}}_{m,k} \mathbf{d}_m \right\|_2^2 + \frac{\sigma_\epsilon^2}{L} \sum_{m=1}^M \sum_{k=1}^M \left\| \tilde{\mathbf{R}}_{m,k} \boldsymbol{\lambda}_m \right\|_2^2, \end{aligned} \quad (3.8)$$

where

$$\begin{aligned} \tilde{\mathbf{R}}_{m,k} &= \text{diag}(r_m(N_1 + kL - L), r_m(N_1 + 1 + kL - L), \dots, r_m(N_1 - 1 + kL)), \\ \mathbf{d}_m &= (d_m(N_1), d_m(N_1 + 1), \dots, d_m(N_1 + L - 1))^T, \\ \mathbf{D}_m &= \text{diag}(\mathbf{d}_m), \\ \boldsymbol{\lambda}_m &= (\lambda_{m,N_1}, \lambda_{m,N_1+1}, \dots, \lambda_{m,L+N_1-1})^T. \end{aligned}$$

Suppose that the matrices and vectors involved in (3.8) are real-valued. To minimize the above expectation of MSE, we denote (3.8) by  $\Phi_2(\boldsymbol{\lambda}_1, \boldsymbol{\lambda}_2, \dots, \boldsymbol{\lambda}_M)$ . Differentiating  $\Phi_2$  with respect to  $\boldsymbol{\lambda}_1, \boldsymbol{\lambda}_2, \dots, \boldsymbol{\lambda}_M$  and solving

$$\nabla_{\boldsymbol{\lambda}_1} \Phi_2 = 0, \nabla_{\boldsymbol{\lambda}_2} \Phi_2 = 0, \dots, \nabla_{\boldsymbol{\lambda}_M} \Phi_2 = 0, \quad (3.9)$$

we can obtain the critical point. Since  $\Phi_2$  is a quadratic function, the critical point gives the unique solution for the optimization problem

$$\min \Phi_2(\boldsymbol{\lambda}_1, \boldsymbol{\lambda}_2, \dots, \boldsymbol{\lambda}_M). \quad (3.10)$$

Observe that the equation (3.9) can be expressed by the following system of linear equations:

$$\boldsymbol{\Psi} \boldsymbol{\lambda} = \boldsymbol{\zeta},$$

where  $\boldsymbol{\Psi}$  is a partitioned matrix with  $M \times M$  blocks,  $\boldsymbol{\lambda}$  and  $\boldsymbol{\zeta}$  are partitioned column vectors with  $M$  blocks, and

$$\begin{aligned} \boldsymbol{\Psi}_{(m,n)} &= \sum_{k=1}^M \mathbf{D}_m \tilde{\mathbf{R}}_{m,k} \tilde{\mathbf{R}}_{n,k} \mathbf{D}_n + \delta(m-n) \frac{\sigma_\epsilon^2}{L} \tilde{\mathbf{R}}_{m,k} \tilde{\mathbf{R}}_{n,k}, \\ \boldsymbol{\lambda}_{(m)} &= \boldsymbol{\lambda}_m, \\ \boldsymbol{\zeta}_{(m)} &= \sum_{k=1}^M \sum_{n=1}^M \mathbf{D}_m \tilde{\mathbf{R}}_{m,k} \tilde{\mathbf{R}}_{n,k} \mathbf{d}_n, \end{aligned}$$

then the solution of (3.10) is given by

$$\boldsymbol{\lambda}^* = \boldsymbol{\Psi}^{-1} \boldsymbol{\zeta}. \quad (3.11)$$

If (3.8) contains complex-valued matrices or vectors, then (3.10) becomes an optimization problem with complex variables. In this case, the objective function can be rewritten as a function of the real and imaginary parts of its complex argument. For any complex matrix  $\mathbf{A} = \mathbf{A}_r + \mathbf{A}_i \mathbf{i} \in \mathbb{C}^{p \times q}$ ,  $\mathbf{A}_r, \mathbf{A}_i \in \mathbb{R}^{p \times q}$ , we define an operator  $\Gamma : \mathbb{C}^{p \times q} \rightarrow \mathbb{R}^{2p \times 2q}$  such that

$$\Gamma(\mathbf{A}) = \begin{bmatrix} \mathbf{A}_r & -\mathbf{A}_i \\ \mathbf{A}_i & \mathbf{A}_r \end{bmatrix} \in \mathbb{R}^{2p \times 2q}.$$



Similarly, for any complex vector  $\mathbf{b} = \mathbf{b}_r + \mathbf{b}_i \mathbf{i} \in \mathbb{C}^p$ ,  $\mathbf{b}_r, \mathbf{b}_i \in \mathbb{R}^p$ , we define an operator  $\gamma : \mathbb{C}^p \rightarrow \mathbb{R}^{2p}$  such that

$$\gamma(\mathbf{b}) = \begin{bmatrix} \mathbf{b}_r \\ \mathbf{b}_i \end{bmatrix} \in \mathbb{R}^{2p}.$$

It can be verified that  $\Gamma$  and  $\gamma$  have the following properties.

- (1)  $\Gamma$  and  $\gamma$  are invertible.
- (2)  $\Gamma(c_1 \mathbf{A} + c_2 \mathbf{B}) = c_1 \Gamma(\mathbf{A}) + c_2 \Gamma(\mathbf{B})$ ,  $\forall c_1, c_2 \in \mathbb{R}, \forall \mathbf{A}, \mathbf{B} \in \mathbb{C}^{p \times q}$ .
- (3)  $\|\gamma(\mathbf{b})\|_2 = \|\mathbf{b}\|_2$ ,  $\forall \mathbf{b} \in \mathbb{C}^p$ .
- (4)  $\gamma(\mathbf{A}\mathbf{b}) = \Gamma(\mathbf{A})\gamma(\mathbf{b})$ ,  $\forall \mathbf{A} \in \mathbb{C}^{p \times q}, \forall \mathbf{b} \in \mathbb{C}^p$ .

By using the defined operators  $\Gamma$  and  $\gamma$ , we can reformulate the objective function as

$$\sum_{k=1}^M \left\| \sum_{m=1}^M \Gamma(\tilde{\mathbf{R}}_{m,k} \mathbf{D}_m) \gamma(\boldsymbol{\lambda}_m) - \gamma(\tilde{\mathbf{R}}_{m,k} \mathbf{d}_m) \right\|_2^2 + \frac{\sigma_\epsilon^2}{L} \sum_{m=1}^M \sum_{k=1}^M \left\| \Gamma(\tilde{\mathbf{R}}_{m,k}) \gamma(\boldsymbol{\lambda}_m) \right\|_2^2.$$

Thus the optimization problem can still be solved by the standard method.

**Remark 3.3** We have provided the closed-form solution for the optimization problem (3.10). If the size of the data is very large, some existing software packages, for example, CVX [15], can also be used to solve the optimization problem.

The formula (3.11) gives the optimal values for the parameters of pre-filtering. To compute  $\boldsymbol{\lambda}^*$ , we have to estimate the value of  $\mathbf{d}_m$  ( $1 \leq m \leq M$ ) from the noisy multichannel samples. In fact, if  $f(t)$  is bandlimited with bandwidth  $\leq N_s$ , then  $\mathbf{d}_\epsilon$  is an unbiased estimation for  $(\mathbf{d}_1; \mathbf{d}_2; \dots; \mathbf{d}_M)$  (see more details in Section 3 of [12]). It is obvious that the spectral density of a function wouldn't change with the sampling schemes in the multichannel reconstruction. For  $\mathbf{d}_m$ , however, it changes with the types and amounts of samples even for a fixed  $f(t)$ , as shown in Table 2. Different from post-filtering, the bandwidth of the reconstructed signal  $\check{f}$  based on pre-filtering equals the number of samples, it can't be adjusted to be equal to the bandwidth of  $f$  by taking specific parameters.

Table 2: The values of  $\mathbf{d}_m$  ( $1 \leq m \leq M$ ) for the test function defined by (3.7) under different sampling schemes.

Sampling schemes	The true values of $\mathbf{d}_m$
$L = 6, M = 1, f$	$\mathbf{d}_1 = (1 + \mathbf{i}, 2 - \mathbf{i}, 1, 2 + \mathbf{i}, 1 - \mathbf{i}, 0)$
$L = 3, M = 2, f, f'$	$\mathbf{d}_1 = (3 + 2\mathbf{i}, 3 - 2\mathbf{i}, 1), \mathbf{d}_2 = (1, 1, 0)$
$L = 3, M = 2, f, \mathcal{H}f$	$\mathbf{d}_1 = (3 + 2\mathbf{i}, 3 - 2\mathbf{i}, 1), \mathbf{d}_2 = (-\mathbf{i}, \mathbf{i}, 0)$
$L = 8, M = 1, f$	$\mathbf{d}_1 = (0, 1 + \mathbf{i}, 2 - \mathbf{i}, 1, 2 + \mathbf{i}, 1 - \mathbf{i}, 0, 0)$
$L = 4, M = 2, f, f'$	$\mathbf{d}_1 = (2 + \mathbf{i}, 2, 2 - \mathbf{i}, 1), \mathbf{d}_2 = (2\mathbf{i} - 1, 4, -1 - 2\mathbf{i}, 0)$
$L = 4, M = 2, f, \mathcal{H}f$	$\mathbf{d}_1 = (2 + \mathbf{i}, 2, 2 - \mathbf{i}, 1), \mathbf{d}_2 = (1 - 2\mathbf{i}, -2, 1 + 2\mathbf{i}, 0)$

### 3.3 A simple comparison between pre-filtering and post-filtering

It can be seen that the model of pre-filtering is more intricate than that of post-filtering. A direct strategy to simplify pre-filtering is enforcing

$$\lambda_1 = \lambda_2 = \cdots = \lambda_M. \quad (3.12)$$

In other words, pre-filtering every channel of samples in the same way. Under this restriction, the objective function becomes

$$\Phi_2(\lambda_0) = \sum_{k=1}^M \left\| \sum_{m=1}^M \tilde{\mathbf{R}}_{m,k} \mathbf{D}_m \lambda_0 - \tilde{\mathbf{R}}_{m,k} \mathbf{d}_m \right\|_2^2 + \frac{\sigma_\epsilon^2}{L} \sum_{m=1}^M \sum_{k=1}^M \left\| \tilde{\mathbf{R}}_{m,k} \lambda_0 \right\|_2^2,$$

where  $\lambda_0 = (\lambda_{N_1}, \lambda_{N_2}, \cdots, \lambda_{L+N_1-1})$ . By the definition of  $r_m$ , we have

$$\sum_{m=1}^M b_m(n + jL - L) r_m(n + kL - L) = \delta(j - k), \quad \forall n \in I_1.$$

It follows that

$$\begin{aligned} & \sum_{m=1}^M d_m(n) r_m(n + kL - L) \\ &= \sum_{m=1}^M \left( \sum_{j=1}^M a(n + jL - L) b_m(n + jL - L) \right) r_m(n + kL - L) \\ &= \sum_{j=1}^M a(n + jL - L) \sum_{m=1}^M b_m(n + jL - L) r_m(n + kL - L) \\ &= \sum_{j=1}^M a(n + jL - L) \delta(j - k) \\ &= a(n + kL - L), \quad \forall n \in I_1. \end{aligned}$$

Therefore

$$\begin{aligned} \sum_{m=1}^M \tilde{\mathbf{R}}_{m,k} \mathbf{d}_m &= (a(N_1 + kL - L), a(N_1 + 1 + kL - L), \cdots, a(N_1 + kL - 1))^T, \\ \tilde{\mathbf{R}}_{m,k} \mathbf{D}_m &= \text{diag} \left( \sum_{m=1}^M \tilde{\mathbf{R}}_{m,k} \mathbf{d}_m \right). \end{aligned}$$

Thus the objective function can be simplified as

$$\Phi_2(\lambda) = \sum_{k=1}^M \sum_{n \in I_1} |a(n + kL - L)(\lambda_n - 1)|^2 + \frac{\sigma_\epsilon^2}{L} \sum_{m=1}^M \sum_{k=1}^M \sum_{n \in I_1} |r_m(n + kL - L) \lambda_n|^2.$$

Recalling the objective function of post-filtering defined by (3.1), we see that the pre-filtering under the condition that  $\lambda_1 = \lambda_2 = \cdots = \lambda_M$  is a special case of post-filtering. This means that pre-filtering and post-filtering have a nontrivial intersection.

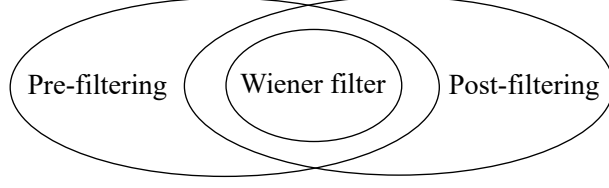


Figure 2: Inclusion relationship of filtering processes

It is noted that if  $M = 1$ , the condition defined by (3.12) is satisfied naturally. When  $M = 1$ , the objective function of post-filtering becomes

$$\Phi_1(\boldsymbol{\beta}) = \sum_{k=K_1}^{K_2} |a(k)(\beta_k - 1)|^2 + \frac{\sigma_\epsilon^2}{L} \sum_{k=K_1}^{K_2} |r_1(k, \text{Type}, N_s)\beta_k|^2.$$

For the sampling scheme F1, we have  $r_1(k, \text{Type}, N_s) = 1$ , then

$$\Phi_1(\boldsymbol{\beta}, \text{F1}) = \sum_{k=K_1}^{K_2} |a(k)(\beta_k - 1)|^2 + \frac{\sigma_\epsilon^2}{L} \sum_{k=K_1}^{K_2} |\beta_k|^2.$$

It follows that

$$\arg \min \Phi_1(\boldsymbol{\beta}, \text{F1}) = \left( |a(k)|^2 \left( |a(k)|^2 + \frac{\sigma_\epsilon^2}{L} \right)^{-1} : K_1 \leq k \leq K_2 \right).$$

It is actually the Wiener filter [16]. By the analysis of Section 3, we see that if  $M = 1$ , the post-filtering is equivalent to the pre-filtering followed by a ideal low-pass filtering. Therefore

$$\arg \min \Phi_2(\boldsymbol{\lambda}, \text{F1}) = \left( |a(k)|^2 \left( |a(k)|^2 + \frac{\sigma_\epsilon^2}{L} \right)^{-1} : N_1 \leq k \leq N_2 \right).$$

From the above discussion, we conclude that the pre-filtering and the post-filtering are two extensions of the Wiener filter in the multichannel reconstruction setting.

### 3.4 Regularized approximation

If the multichannel samples  $\mathbf{s}_1, \mathbf{s}_2, \dots, \mathbf{s}_M$  are noiseless. The goal of reconstruction is to find a function  $\tilde{f}(t)$  such that the residual  $\sum_{m=1}^M \|\tilde{\mathbf{g}}_m - \mathbf{s}_m\|$  is small, where

$$\tilde{\mathbf{g}}_m = \left( \tilde{f} * h_m(t_0), \tilde{f} * h_m(t_1), \dots, \tilde{f} * h_m(t_{L-1}) \right)^T, \quad t_p = \frac{2\pi p}{L}, 1 \leq m \leq M.$$

That is, to solve the optimization problem:

$$\text{minimize } \sum_{m=1}^M \|\tilde{\mathbf{g}}_m - \mathbf{s}_m\|$$

with respect to  $\tilde{f}$ . If the multichannel samples are noisy, it is desirable that a small variation in  $\mathbf{s}_m$  ( $1 \leq m \leq M$ ) would not cause a large variation in  $\tilde{f}$ . Generally, however, the optimal value

of the above optimization problem is sensitive to the data  $\mathbf{s}_m$  ( $1 \leq m \leq M$ ). A common used approach to deal with the sensitivity is to add a penalty term  $\varphi(\tilde{f})$  in optimization [17]. Consequently, the reconstruction problem can be described as a optimization problem of minimizing a weighted sum of two objectives:

$$\text{minimize } \sum_{m=1}^M \|\tilde{\mathbf{g}}_m - \mathbf{s}_m\| + \alpha\varphi(\tilde{f}).$$

Suppose that

$$\tilde{f}(t) = \sum_{n=N_1}^{N_2} x(n)e^{int},$$

we rewrite the above optimization problem as follows:

$$\text{minimize } \sum_{m=1}^M \|\mathbf{C}_m \mathbf{x} - \mathbf{s}_m\|_2^2 + \alpha\varphi(\mathbf{x}),$$

where  $\mathbf{x} = (x(N_1), x(N_1 + 1), \dots, x(N_2))^T$  and

$$\mathbf{C}_m = \begin{bmatrix} b_m(N_1)e^{iN_1t_0} & b_m(N_1 + 1)e^{i(N_1+1)t_0} & \dots & b_m(N_2)e^{iN_2t_0} \\ b_m(N_1)e^{iN_1t_1} & b_m(N_1 + 1)e^{i(N_1+1)t_1} & \dots & b_m(N_2)e^{iN_2t_1} \\ \vdots & \vdots & & \vdots \\ b_m(N_1)e^{iN_1t_{L-1}} & b_m(N_1 + 1)e^{i(N_1+1)t_{L-1}} & \dots & b_m(N_2)e^{iN_2t_{L-1}} \end{bmatrix}.$$

The key problem is how to design the penalty term  $\varphi$  that brings robustness to the reconstruction.

Let

$$\mathbf{W}_\eta = \text{diag}(1 + |N_1|^\eta, 1 + |N_1 + 1|^\eta, \dots, 1 + |N_2|^\eta)$$

be a weighting matrix, we consider the following penalties:

$$\varphi_1(\mathbf{x}) = \sigma_\epsilon^2 \|\mathbf{W}_\eta \mathbf{x}\|_1, \quad \varphi_2(\mathbf{x}) = \sigma_\epsilon^2 \|\mathbf{W}_\eta \mathbf{x}\|_2^2.$$

The role of  $\mathbf{W}_\eta$  is to suppress the high frequency to achieve smoothing, and the parameter  $\eta$  is used to control the amount of smoothness. The  $l_1$ -norm appeared in  $\varphi_1(\mathbf{x})$  induces sparsity [18] for the spectral of  $\tilde{f}$ . The hypothesis of sparsity is based on the priori knowledge that the actual effective information of a signal  $f$  is concentrated in a low-dimensional space even if it is high dimensional. The other penalty term  $\varphi_2(\mathbf{x})$  is a common form of regularization based on the  $l_2$ -norm, say Tikhonov regularization. This regularization results in a quadratic optimization problem, thus enabling an explicit solution.

By using the operators  $\Gamma$  and  $\gamma$ , the objective function of the  $l_2$  regularization can be rewritten as

$$\sum_{m=1}^M \|\Gamma(\mathbf{C}_m) \gamma(\mathbf{x}) - \gamma(\mathbf{s}_m)\|_2^2 + \alpha\sigma_\epsilon^2 \|\Gamma(\mathbf{W}_\eta) \gamma(\mathbf{x})\|_2^2.$$

To solve the optimization problem of the  $l_1$  regularization with complex variables, we need to use the permutation matrix  $\mathbf{P}_K$  corresponding to the permutation

$$(1, 2, \dots, K) \mapsto (1, \frac{K}{2} + 1, 2, \frac{K}{2} + 2, \dots, \frac{K}{2}, K),$$

where  $K$  is an even number. Let  $\mathbf{y} = \mathbf{W}_\eta \mathbf{x}$ , then the objective function

$$\sum_{m=1}^M \|\mathbf{C}_m \mathbf{x} - \mathbf{s}_m\|_2^2 + \alpha \sigma_\epsilon^2 \|\mathbf{W}_\eta \mathbf{x}\|_1$$

becomes

$$\begin{aligned} & \sum_{m=1}^M \|\mathbf{C}_m \mathbf{W}_\eta^{-1} \mathbf{y} - \mathbf{s}_m\|_2^2 + \alpha \sigma_\epsilon^2 \|\mathbf{y}\|_1 \\ &= \sum_{m=1}^M \|\Gamma(\mathbf{C}_m \mathbf{W}_\eta^{-1}) \gamma(\mathbf{y}) - \gamma(\mathbf{s}_m)\|_2^2 + \alpha \sigma_\epsilon^2 \|\mathbf{y}\|_1 \end{aligned}$$

Let  $\mathbf{y}^{(p)} = \mathbf{P}_K \gamma(\mathbf{y})$  and we partition  $\mathbf{y}^{(p)}$  to be  $(\mathbf{y}_1^{(p)}; \mathbf{y}_2^{(p)}; \dots; \mathbf{y}_{\frac{K}{2}}^{(p)})$ , where  $\mathbf{y}_k^{(p)} \in \mathbb{R}^2$ ,  $1 \leq k \leq \frac{K}{2}$ . Namely, we view  $\mathbf{y}^{(p)}$  as a partitioned column vector and its  $k$ -th block is a two dimensional vector  $\mathbf{y}_k^{(p)}$ . By the definition of  $\mathbf{y}^{(p)}$  and using the operator  $\gamma$ , we have that

$$\|\mathbf{y}\|_1 = \sum_{k=1}^{K/2} \|\mathbf{y}_k^{(p)}\|_2.$$

Thus, the objective function of the  $l_1$  regularization can be rewritten as

$$\sum_{m=1}^M \|\Gamma(\mathbf{C}_m \mathbf{W}_\eta^{-1}) \mathbf{P}_K^T \mathbf{y}^{(p)} - \gamma(\mathbf{s}_m)\|_2^2 + \alpha \sigma_\epsilon^2 \sum_{k=1}^{K/2} \|\mathbf{y}_k^{(p)}\|_2.$$

It is actually a sum-of-norms regularization problem [19] and it can be solved by the Alternating Direction Method of Multipliers (ADMM) framework [20].

## 4 Theoretical convergence analysis of post-filtering

First, we assume that  $f \in B_{\mathbf{K}}$ ,  $I^{\mathbf{K}} = \{k, K_1 \leq k \leq K_2\}$  and  $\mu(I^{\mathbf{K}}) \leq \mu(I^{\mathbf{N}}) = N_s$ , where  $N_s$  is the total number of samples. Let  $w(t) \in B_{\mathbf{K}}$ . The minimum value of  $\Phi_1(\boldsymbol{\beta}, F1)$  is equal to

$$\Phi_1(\boldsymbol{\beta}^*, F1) = \sum_{k=K_1}^{K_2} \frac{|a(k)|^2 \sigma_\epsilon^2}{|a(k)|^2 \cdot L + \sigma_\epsilon^2}.$$

It follows that

$$\lim_{L \rightarrow \infty} \Phi_1(\boldsymbol{\beta}^*, F1) = 0.$$

Similarly,

$$\lim_{L \rightarrow \infty} \Phi_2(\boldsymbol{\lambda}_0^*, F1) = 0.$$

Using the previously computed  $r_m$  for FH2 and FD2, we have that

$$\Phi_1(\boldsymbol{\beta}^*, FH2) = \frac{2|a(0)|^2 \sigma_\epsilon^2}{|a(0)|^2 L + 2\sigma_\epsilon^2} + \sum_{K_1 \leq k \leq K_2, k \neq 0} \frac{|a(k)|^2 \sigma_\epsilon^2}{2|a(k)|^2 L + \sigma_\epsilon^2},$$

and

$$\Phi_1(\beta^*, \text{FD2}) = \sum_{k=K_1}^{K_2} \frac{|a(k)|^2 (1 + (L - |k|)^2) \sigma_\epsilon^2}{|a(k)|^2 L^3 + (1 + (L - |k|)^2) \sigma_\epsilon^2}.$$

We see that both  $\Phi_1(\beta^*, \text{FH2})$  and  $\Phi_1(\beta^*, \text{FD2})$  are convergent to 0 as  $L \rightarrow \infty$ .

An important choice of  $w(t)$  for post-filtering is  $D(t, K_1, K_2)$  defined by (2.2), an analogue of the ideal low-pass filter. Note that

$$f * D(\cdot, K_1, K_2)(t) = f(t)$$

provided that  $f \in B_{\mathbf{K}}$ . It follows that

$$\begin{aligned} \tilde{f}(t, N_s, \mathbf{K}) - f(t) &= f_{\mathbf{N}, \epsilon} * D(\cdot, K_1, K_2)(t) - f * D(\cdot, K_1, K_2)(t) \\ &= ((f_{\mathbf{N}, \epsilon} - f) * D(\cdot, K_1, K_2))(t) \\ &= \frac{1}{L} \sum_{m=1}^M \sum_{p=0}^{L-1} \epsilon_{m,p} (y_m * D(\cdot, K_1, K_2)) \left(t - \frac{2\pi p}{L}\right). \end{aligned}$$

Since  $\{\epsilon_{m,p}\}$  is an i.i.d. noise process, we have that

$$\begin{aligned} &\mathbb{E} \left| \tilde{f}(t, N_s, \mathbf{K}) - f(t) \right|^2 \\ &= \frac{1}{L^2} \sum_{m=1}^M \sum_{p=0}^{L-1} \left| (y_m * D(\cdot, K_1, K_2)) \left(t - \frac{2\pi p}{L}\right) \right|^2 \mathbb{E}[\epsilon_{m,p}^2] \\ &= \frac{1}{L^2} \sum_{m=1}^M \sum_{p=0}^{L-1} \left| (y_m * D(\cdot, K_1, K_2)) \left(t - \frac{2\pi p}{L}\right) \right|^2 \sigma_\epsilon^2. \end{aligned}$$

Therefore

$$\begin{aligned} &\mathbb{E} \left( \frac{1}{2\pi} \int_0^{2\pi} \left| \tilde{f}(t, N_s, \mathbf{K}) - f(t) \right|^2 dt \right) \\ &= \frac{1}{2\pi} \int_0^{2\pi} \mathbb{E} \left| \tilde{f}(t, N_s, \mathbf{K}) - f(t) \right|^2 dt \\ &= \frac{\sigma_\epsilon^2}{L^2} \sum_{m=1}^M \sum_{p=0}^{L-1} \frac{1}{2\pi} \int_0^{2\pi} \left| (y_m * D(\cdot, K_1, K_2)) \left(t - \frac{2\pi p}{L}\right) \right|^2 dt \\ &= \frac{\sigma_\epsilon^2}{L} \sum_{m=1}^M \|y_m * D(\cdot, K_1, K_2)\|_2^2 = \frac{\sigma_\epsilon^2}{L} \sum_{m=1}^M \sum_{n \in I^{\mathbf{K}}} |r_m(n, \text{Type}, N_s)|^2. \end{aligned}$$

We examine the accuracy of the reconstructed signal  $\tilde{f}(t, N_s, \mathbf{K})$  for sampling schemes F1, FH2 and FD2. Without loss of generality, let  $\mu(I^{\mathbf{K}}) = 2K_2$ ,  $K_1 = 1 - K_2$ , we have that

$$\begin{aligned} \frac{\sigma_\epsilon^2}{L} \sum_{m=1}^M \sum_{n \in I^{\mathbf{K}}} |r_m(n, \text{F1}, N_s)|^2 &= \frac{2K_2 \sigma_\epsilon^2}{N_s}, \\ \frac{\sigma_\epsilon^2}{L} \sum_{m=1}^M \sum_{n \in I^{\mathbf{K}}} |r_m(n, \text{FH2}, N_s)|^2 &= \frac{(2K_2 + 3) \sigma_\epsilon^2}{N_s}, \end{aligned}$$

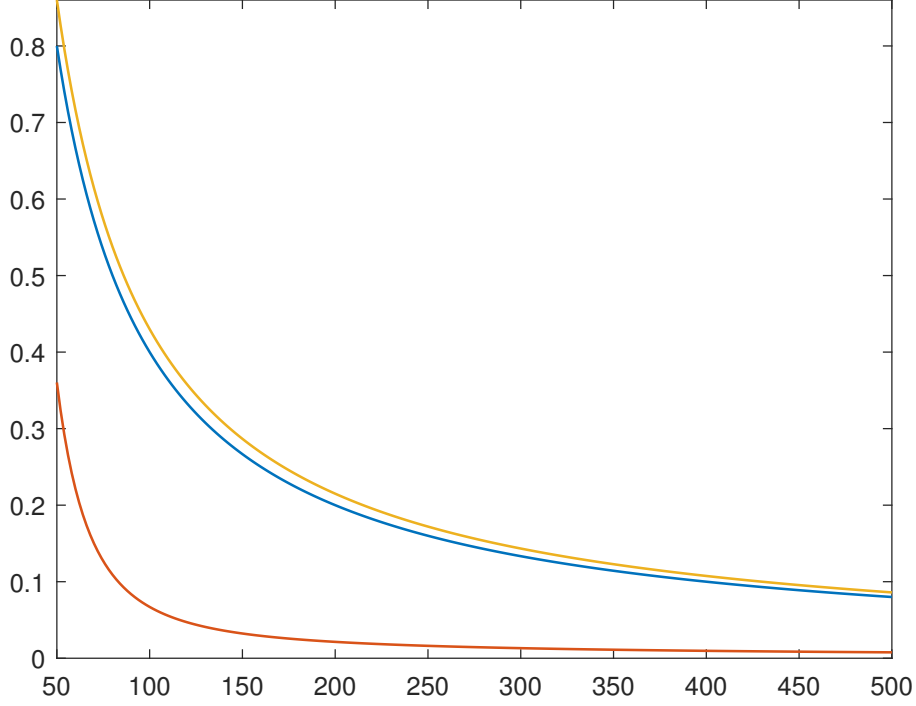


Figure 3: Plot of  $\frac{\sigma_\epsilon^2}{L} \sum_{m=1}^M \sum_{n \in I^{\mathbf{K}}} |r_m(n, \text{Type}, N_s)|^2$  with  $K_2 = 20$  for F1 (blue), FH2 (yellow) and FD2 (orange). The horizontal axis represents the total number of samples  $N_s$ .

$$\frac{\sigma_\epsilon^2}{L} \sum_{m=1}^M \sum_{n \in I^{\mathbf{K}}} |r_m(n, \text{FD2}, N_s)|^2 = \frac{4\sigma_\epsilon^2}{N_s} + \frac{56K_2\sigma_\epsilon^2}{3N_s^3} + \frac{16K_2^3\sigma_\epsilon^2}{3N_s^3} - \frac{8K_2\sigma_\epsilon^2}{N_s^2}.$$

It is easy to see that  $\frac{\sigma_\epsilon^2}{L} \sum_{m=1}^M \sum_{n \in I^{\mathbf{K}}} |r_m(n, \text{Type}, N_s)|^2 \rightarrow 0$  as  $N_s \rightarrow \infty$ . As for different sampling schemes, FD2 performs better than F1 and FH2.

**Remark 4.1** *To examine the convergence property of the optimal post-filtering for the sampling schemes in addition to F1, FH2 and FD2, one can consider firstly the post-filtering by the Dirichlet kernel for its simplicity, since the expectation of MSE for the optimal post-filtering is always no larger than that of post-filtering by the Dirichlet kernel.*

To analyze the convergence of post-filtering for the non-bandlimited signal, we need the following lemmas.

**Lemma 4.2** *If  $f \in C^j(\mathbb{T})$ , then there exists a constant  $\gamma$  such that  $|a(n)| \leq \gamma/|n|^j$  for  $n \neq 0$ .*

**Lemma 4.3** *Let  $c_k = \sum_{n=k+1}^{\infty} n^{-\alpha}$  with  $\alpha > 1$ , then*

$$(\alpha - 1)^{-1}(k + 1)^{1-\alpha} < c_k < (\alpha - 1)^{-1}k^{1-\alpha}$$

for all  $k \in \mathbb{Z}^+$ .

**Proof.** Since  $\alpha > 1$ , then  $x^{-\alpha}$  is a monotonic decreasing function on  $(0, +\infty)$ . It follows that

$$\int_{k+1}^{\infty} x^{-\alpha} dx < \sum_{n=k+1}^{\infty} \frac{1}{n^\alpha} < \int_k^{\infty} x^{-\alpha} dx, \quad \forall k \in \mathbb{Z}^+.$$

Note that  $\int_{k+1}^{\infty} x^{-\alpha} dx = (\alpha - 1)^{-1}(k + 1)^{1-\alpha}$  and  $\int_k^{\infty} x^{-\alpha} dx = (\alpha - 1)^{-1}k^{1-\alpha}$ , the proof is complete.  $\square$

If  $f$  is non-bandlimited, the error of the reconstruction for  $f$  by post-filtering comes from not only noise but also aliasing. Let  $c_k = \sum_{|n| \geq k+1} |a(n)|^2$ , where  $a(n)$  is the Fourier coefficient of  $f$ . Then  $c_k$  tends to 0 as  $k \rightarrow \infty$  under the assumption that  $f \in L^2(\mathbb{T})$ . By Lemmas 4.2 and 4.3, we see that the convergence rate of  $c_k \rightarrow 0$  can be very fast if  $f$  is smooth. It is known that if the number of samples  $N_s$  is sufficient large such that  $c_K$  ( $K = (N_s - 1)/2$ ) is sufficient small, then the aliasing error is negligible. Therefore, if we take sufficient large  $K_1, K_2$  in post-filtering, the aliasing error can be sufficient small.

For pre-filtering and regularized approximation, there is no guarantee that the expectation of MSE will tend to 0 when the number of samples goes to infinity. Nonetheless, it doesn't mean that the performance of post-filtering is better than pre-filtering and regularized approximation in signal reconstruction when the number of samples is finite. It is important to clarify whether the reconstruction results using smoothing corrections would converge to the original signal as the number of samples tends to infinity. In practice, however, the total number of samples is finite. Therefore, we need to examine which of the aforementioned methods can achieve preferable reconstruction results under the same sample set of limited size. Besides, it is necessary to test whether combining pre-filtering and post-filtering could give some distinctive results. In the next section, the proposed smoothing and regularization strategies are verified comprehensively by a number of numerical simulations.

## 5 Numerical simulations

In the last section we introduced three smoothing strategies to reduce the effect of noise in multichannel reconstruction. To provide a more intuitive understanding of the above theoretical analysis, we give a number of examples to show the exact formulas of the proposed smoothing strategies in some concrete sampling schemes.

Recall  $\phi(z)$  defined by (2.1), we use  $f(t) = \phi(e^{it})$  as the test function. Obviously,  $f(t)$  is non-bandlimited. To use the proposed post-filtering, a suitable choice of  $K_1$  and  $K_2$  is needed. Given a set of noisy multichannel samples, an estimate for  $|a(n)|^2$  is obtained by applying the estimation method for the spectral density (see Section 3.1.2). Then we take the smallest possible  $\tilde{K}_1, \tilde{K}_2$  (absolute value) such that

$$\frac{\sum_{n=\tilde{K}_1}^{\tilde{K}_2} \tilde{A}(n)}{\sum_n \tilde{A}(n)} \geq 0.9, \quad (5.1)$$

where  $\tilde{A}(n)$  is the estimate for  $|a(n)|^2$ . The selection of  $\tilde{\mathbf{K}} = \{n : \tilde{K}_1 \leq n \leq \tilde{K}_2\}$  is diagramed in Figure 4. If the number of samples is sufficiently large, the bandwidth of the post-filter can be increased properly. Thus the final selection of the bandwidth for post-filtering is

$$\mu(I^{\mathbf{K}}) = \max\{2\sqrt{N_s}, \mu(I^{\tilde{\mathbf{K}}})\}.$$

As for the parameters of  $l_1$  and  $l_2$  regularization, the experiential values are  $\eta = 1.2$  and  $\alpha = 1$ . It is hard to make out which set of parameters  $\eta, \alpha$  is the best due to the limited information



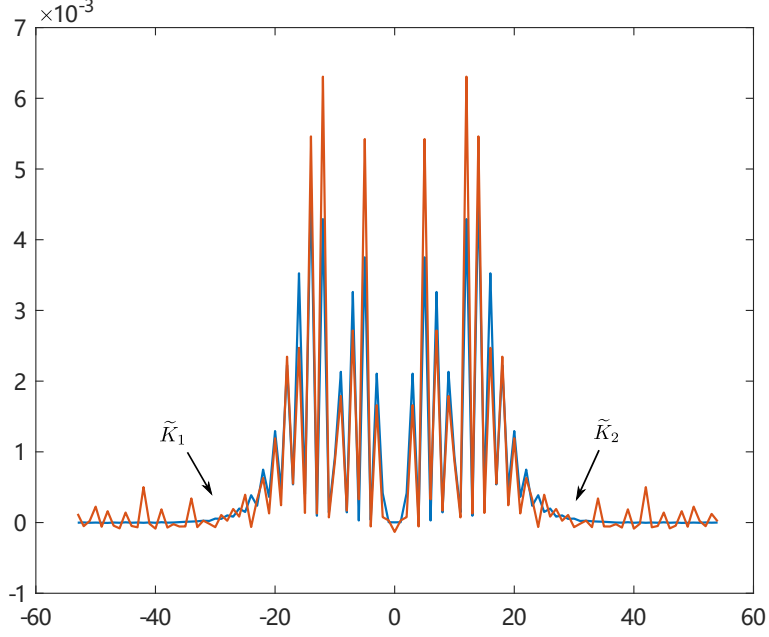


Figure 4: The blue line is the true value of  $|a(n)|^2$ . The orange line is the estimated spectral density  $\tilde{A}(n)$  from 54 noisy samples of  $f$  and 54 noisy samples of  $\mathcal{H}f$ . The experiential values for  $\tilde{K}_1, \tilde{K}_2$  can be set as the inflection points where  $\tilde{A}(n)$  tapers off to zero.

of the signal acquired. But they can be tuned using the estimated spectral density. Roughly speaking, the faster decline of  $\tilde{A}(n)$ , the larger  $\eta$ ; the sparser of  $\tilde{A}(n)$ , the larger  $\alpha$ .

The experiments are conducted to compare the reconstructed results by the proposed methods under the sampling schemes of F1, FH2 and FD2. The Gaussian noise with standard deviation 0.05 are superposed on the samples of F1 and FH2. While the samples of FD2 are corrupted by the Gaussian noise with standard deviation 0.1. The expectation of mean square error (EMSE) is approximated by the average of mean square error over 10000 times experiments. The EMSEs for the reconstructions in different situations are listed in Table 3, 4 and 5. Besides, Table 6 reports the running time for the reconstruction under the sampling scheme of FD2 in detail. Furthermore, the reconstructed results by the proposed methods under the sampling scheme of FD2 with  $N_s = 1248$  is From the results we make the following conclusions.

1. The experimental results prove that all the reconstruction methods based on smoothing or regularization have improved in terms of accuracy compared to the MCI. Moreover, the errors of reconstruction reduce with the increase of the size of samples.
2. If the sample size is small, the composite of pre-filtering and post-filtering is effective. The double-stage filtering can remove noise in the multichannel reconstruction to a large extent.
3. If the number of samples is relatively large, the capability of noise removal of pre-filtering is insufficient (see Figure 5). Whereas, using only the post-filtering can achieve a good performance in noise reduction.
4. Although the errors of reconstruction by  $l_1$  and  $l_2$  regularization are relatively small, the corresponding reconstructed signals look a bit rough if no post-filtering is performed (see

Figure 5). The  $l_1$  or  $l_2$  regularization followed by post-filtering can achieve a slightly better performance than just using post-filtering. This improvement comes at the expense of high computational complexity. For example, when  $N_s = 1248$ ,  $l_1$  regularization spend at least 1000 times as much time as post-filtering on the reconstruction (see Table 6).

We have proved the convergence of post-filtering theoretically. This implies that the reconstructed signal obtained by post-filtering will converge to  $f$  provided that the true value of  $|a(n)|^2$  is available. In a real application, however, we can only use the estimate of  $|a(n)|^2$ , i.e.,  $\tilde{A}(n)$ , to perform post-filtering. It has been shown that the more samples taken in reconstruction, the more accurate the spectral density estimate. Thus it is not surprising that the error of reconstruction by post-filtering tends to zero as the number of samples tends to infinity in practice. Moreover, as can be seen from Figure 6 that the errors of reconstruction by pre-filtering,  $l_1$  and  $l_2$  regularization in combination with post-filtering are also convergent to 0 as  $N_s \rightarrow \infty$ .

The above analysis suggests that the composite of pre-filtering and post-filtering is preferable to the other methods when the sample size is small. Otherwise, post-filtering a good choice because it could produce a fine result in a relatively short period. If one does not give a high priority to the execution time,  $l_1$  (or  $l_2$ ) regularization combined with post-filtering has the capability to achieve a remarkable reconstruction result provided that suitable parameters are selected.

## 6 Conclusion and discussion

In this paper, we propose several smoothing and regularization based methods to reconstruct signal from its multichannel samples in the presence of noise. The experiments show that the proposed methods can be effectively used to reduce the error caused by noise in multichannel reconstruction under limited size of samples. Moreover, we also develop the theoretical and experimental convergence analysis to ensure the high precision in reconstruction under large-scale samples. In addition, some operators are devised to tackle the optimization problems with complex variables such that they can be solved by the standard algorithms.

The proposed methods are established under the MSE criterion which is suitable for the Gaussianity assumption of noise distribution. Because maximum correntropy criterion (MCC) is independent of the noise distribution, it has been used to deal with the samples corrupted by non-Gaussian noise [21]. To cope with various types of noises, therefore, there is a great need to develop smoothing and regularization based methods for multichannel reconstruction through minimizing correntropy induced metric (CIM). This topic will be discussed in our further studies.

Table 3: The EMSEs of the reconstruction from the noisy samples of  $f$  and  $\mathcal{H}f$  by different methods. The standard deviation of the noise is  $\sigma_\epsilon = 0.05$ . The parameters of  $l_1$  regularization and  $l_2$  regularization are  $\eta = 1.2, \alpha = 1$ .

No. of $S$	MCI	MCI+ Post-filt	Pre-filt +MCI	Pre-filt +MCI+ Post-filt	$l_1$ -Reg	$l_1$ -Reg+ Post-filt	$l_2$ -Reg	$l_2$ -Reg+ Post-filt
12	$1.9775 \cdot 10^{-1}$	$1.9552 \cdot 10^{-1}$	$1.9658 \cdot 10^{-1}$	<b><math>1.9511 \cdot 10^{-1}</math></b>	$1.9613 \cdot 10^{-1}$	$1.9613 \cdot 10^{-1}$	$1.9662 \cdot 10^{-1}$	$1.9662 \cdot 10^{-1}$
24	$1.1846 \cdot 10^{-1}$	$1.1686 \cdot 10^{-1}$	$1.1647 \cdot 10^{-1}$	<b><math>1.1533 \cdot 10^{-1}</math></b>	$1.1770 \cdot 10^{-1}$	$1.1770 \cdot 10^{-1}$	$1.1786 \cdot 10^{-1}$	$1.1786 \cdot 10^{-1}$
36	$3.4946 \cdot 10^{-2}$	<b><math>3.3460 \cdot 10^{-2}</math></b>	$3.4789 \cdot 10^{-2}$	$3.3491 \cdot 10^{-2}$	$3.4673 \cdot 10^{-2}$	$3.4673 \cdot 10^{-2}$	$3.4600 \cdot 10^{-2}$	$3.4600 \cdot 10^{-2}$
48	$7.9627 \cdot 10^{-3}$	$7.3021 \cdot 10^{-3}$	$7.7302 \cdot 10^{-3}$	<b><math>7.2938 \cdot 10^{-3}</math></b>	$7.8393 \cdot 10^{-3}$	$7.8393 \cdot 10^{-3}$	$7.7912 \cdot 10^{-3}$	$7.7912 \cdot 10^{-3}$
60	$3.2912 \cdot 10^{-3}$	$3.0928 \cdot 10^{-3}$	<b><math>2.9815 \cdot 10^{-3}</math></b>	$3.1310 \cdot 10^{-3}$	$3.1743 \cdot 10^{-3}$	$3.1743 \cdot 10^{-3}$	$3.1252 \cdot 10^{-3}$	$3.1252 \cdot 10^{-3}$
72	$2.6287 \cdot 10^{-3}$	$2.4180 \cdot 10^{-3}$	<b><math>2.2175 \cdot 10^{-3}</math></b>	$2.4221 \cdot 10^{-3}$	$2.4276 \cdot 10^{-3}$	$2.4276 \cdot 10^{-3}$	$2.4091 \cdot 10^{-3}$	$2.4091 \cdot 10^{-3}$
84	$2.5423 \cdot 10^{-3}$	$2.0685 \cdot 10^{-3}$	$2.2424 \cdot 10^{-3}$	$2.2205 \cdot 10^{-3}$	$2.2442 \cdot 10^{-3}$	$2.0622 \cdot 10^{-3}$	$2.2607 \cdot 10^{-3}$	<b><math>2.0336 \cdot 10^{-3}</math></b>
96	$2.5282 \cdot 10^{-3}$	$1.8273 \cdot 10^{-3}$	$2.3179 \cdot 10^{-3}$	$2.0671 \cdot 10^{-3}$	$2.1484 \cdot 10^{-3}$	$1.8150 \cdot 10^{-3}$	$2.2024 \cdot 10^{-3}$	<b><math>1.8018 \cdot 10^{-3}</math></b>
108	$2.5250 \cdot 10^{-3}$	$1.6405 \cdot 10^{-3}$	$2.3580 \cdot 10^{-3}$	$1.9529 \cdot 10^{-3}$	$2.0835 \cdot 10^{-3}$	$1.6371 \cdot 10^{-3}$	$2.1542 \cdot 10^{-3}$	<b><math>1.6231 \cdot 10^{-3}</math></b>
120	$2.5211 \cdot 10^{-3}$	$1.4869 \cdot 10^{-3}$	$2.3664 \cdot 10^{-3}$	$1.8617 \cdot 10^{-3}$	$2.0206 \cdot 10^{-3}$	$1.4721 \cdot 10^{-3}$	$2.0960 \cdot 10^{-3}$	<b><math>1.4635 \cdot 10^{-3}</math></b>
168	$2.5164 \cdot 10^{-3}$	$1.1042 \cdot 10^{-3}$	$2.1058 \cdot 10^{-3}$	$1.4307 \cdot 10^{-3}$	$1.8323 \cdot 10^{-3}$	<b><math>1.0761 \cdot 10^{-3}</math></b>	$1.9180 \cdot 10^{-3}$	<b><math>1.0761 \cdot 10^{-3}</math></b>
216	$2.5129 \cdot 10^{-3}$	$8.8555 \cdot 10^{-4}$	$1.8827 \cdot 10^{-3}$	$1.1820 \cdot 10^{-3}$	$1.6987 \cdot 10^{-3}$	<b><math>8.4862 \cdot 10^{-4}</math></b>	$1.7668 \cdot 10^{-3}$	$8.5065 \cdot 10^{-4}$
264	$2.5098 \cdot 10^{-3}$	$7.3196 \cdot 10^{-4}$	$1.7338 \cdot 10^{-3}$	$9.7474 \cdot 10^{-4}$	$1.5784 \cdot 10^{-3}$	$7.0312 \cdot 10^{-4}$	$1.6337 \cdot 10^{-3}$	<b><math>6.9867 \cdot 10^{-4}</math></b>
312	$2.5089 \cdot 10^{-3}$	$6.3254 \cdot 10^{-4}$	$1.6276 \cdot 10^{-3}$	$8.6721 \cdot 10^{-4}$	$1.4790 \cdot 10^{-3}$	$6.0003 \cdot 10^{-4}$	$1.5259 \cdot 10^{-3}$	<b><math>5.9896 \cdot 10^{-4}</math></b>
624	$2.5054 \cdot 10^{-3}$	$3.3926 \cdot 10^{-4}$	$1.3195 \cdot 10^{-3}$	$5.1712 \cdot 10^{-4}$	$1.0687 \cdot 10^{-3}$	<b><math>3.1818 \cdot 10^{-4}</math></b>	$1.0924 \cdot 10^{-3}$	$3.1880 \cdot 10^{-4}$
1248	$2.5017 \cdot 10^{-3}$	$1.8626 \cdot 10^{-4}$	$1.1503 \cdot 10^{-3}$	$3.2887 \cdot 10^{-4}$	$7.1142 \cdot 10^{-4}$	$1.7610 \cdot 10^{-4}$	$7.4592 \cdot 10^{-4}$	<b><math>1.7548 \cdot 10^{-4}</math></b>

Table 4: The EMSEs of reconstruction from the noisy samples of  $f$  and  $f'$  by different methods. The standard deviation of the noise is  $\sigma_\epsilon = 0.1$ . The parameters of  $l_1$  regularization and  $l_2$  regularization are  $\eta = 1.2, \alpha = 1$ .

No. of $S$	MCI	MCI+ Post-filt	Pre-filt +MCI	Pre-filt +MCI+ Post-filt	$l_1$ -Reg	$l_1$ -Reg+ Post-filt	$l_2$ -Reg	$l_2$ -Reg+ Post-filt
12	$2.0447 \cdot 10^{-1}$	$1.9696 \cdot 10^{-1}$	$1.9810 \cdot 10^{-1}$	<b><math>1.9187 \cdot 10^{-1}</math></b>	$2.0228 \cdot 10^{-1}$	$2.0228 \cdot 10^{-1}$	$2.0193 \cdot 10^{-1}$	$2.0193 \cdot 10^{-1}$
24	$1.6772 \cdot 10^{-1}$	$1.6002 \cdot 10^{-1}$	$1.6298 \cdot 10^{-1}$	<b><math>1.5505 \cdot 10^{-1}</math></b>	$1.6606 \cdot 10^{-1}$	$1.6606 \cdot 10^{-1}$	$1.6646 \cdot 10^{-1}$	$1.6646 \cdot 10^{-1}$
36	$6.3027 \cdot 10^{-2}$	$5.8539 \cdot 10^{-2}$	$5.9992 \cdot 10^{-2}$	<b><math>5.7333 \cdot 10^{-2}</math></b>	$6.1093 \cdot 10^{-2}$	$6.1093 \cdot 10^{-2}$	$6.1223 \cdot 10^{-2}$	$6.1223 \cdot 10^{-2}$
48	$1.7364 \cdot 10^{-2}$	<b><math>1.5195 \cdot 10^{-2}</math></b>	$1.5838 \cdot 10^{-2}$	$1.5500 \cdot 10^{-2}$	$1.6414 \cdot 10^{-2}$	$1.6414 \cdot 10^{-2}$	$1.6276 \cdot 10^{-2}$	$1.6276 \cdot 10^{-2}$
60	$8.3509 \cdot 10^{-3}$	<b><math>7.0806 \cdot 10^{-3}</math></b>	$7.4106 \cdot 10^{-3}$	$7.8499 \cdot 10^{-3}$	$7.7873 \cdot 10^{-3}$	$7.7873 \cdot 10^{-3}$	$7.8924 \cdot 10^{-3}$	$7.8924 \cdot 10^{-3}$
72	$6.9644 \cdot 10^{-3}$	$6.0299 \cdot 10^{-3}$	<b><math>5.9683 \cdot 10^{-3}</math></b>	$6.8682 \cdot 10^{-3}$	$6.5291 \cdot 10^{-3}$	$6.5291 \cdot 10^{-3}$	$6.6630 \cdot 10^{-3}$	$6.6630 \cdot 10^{-3}$
84	$6.7706 \cdot 10^{-3}$	$6.0350 \cdot 10^{-3}$	<b><math>5.9369 \cdot 10^{-3}</math></b>	$7.0210 \cdot 10^{-3}$	$6.2032 \cdot 10^{-3}$	$6.2061 \cdot 10^{-3}$	$6.3276 \cdot 10^{-3}$	$6.3296 \cdot 10^{-3}$
96	$6.7236 \cdot 10^{-3}$	$5.9158 \cdot 10^{-3}$	$5.9449 \cdot 10^{-3}$	$6.8447 \cdot 10^{-3}$	$5.8551 \cdot 10^{-3}$	<b><math>5.7939 \cdot 10^{-3}</math></b>	$6.0500 \cdot 10^{-3}$	$5.9837 \cdot 10^{-3}$
108	$6.6940 \cdot 10^{-3}$	$5.7642 \cdot 10^{-3}$	$5.9548 \cdot 10^{-3}$	$6.6695 \cdot 10^{-3}$	$5.5846 \cdot 10^{-3}$	<b><math>5.4172 \cdot 10^{-3}</math></b>	$5.8015 \cdot 10^{-3}$	$5.6187 \cdot 10^{-3}$
120	$6.6832 \cdot 10^{-3}$	$5.6607 \cdot 10^{-3}$	$5.8638 \cdot 10^{-3}$	$6.5043 \cdot 10^{-3}$	$5.2678 \cdot 10^{-3}$	<b><math>4.9812 \cdot 10^{-3}</math></b>	$5.6014 \cdot 10^{-3}$	$5.2933 \cdot 10^{-3}$
168	$6.6281 \cdot 10^{-3}$	$4.4436 \cdot 10^{-3}$	$5.2445 \cdot 10^{-3}$	$4.7156 \cdot 10^{-3}$	$4.5830 \cdot 10^{-3}$	<b><math>4.0760 \cdot 10^{-3}</math></b>	$4.9211 \cdot 10^{-3}$	$4.2980 \cdot 10^{-3}$
216	$6.6302 \cdot 10^{-3}$	$3.7970 \cdot 10^{-3}$	$4.9550 \cdot 10^{-3}$	$3.8718 \cdot 10^{-3}$	$4.0361 \cdot 10^{-3}$	<b><math>3.4458 \cdot 10^{-3}</math></b>	$4.4431 \cdot 10^{-3}$	$3.6661 \cdot 10^{-3}$
264	$6.6175 \cdot 10^{-3}$	$3.4145 \cdot 10^{-3}$	$4.7180 \cdot 10^{-3}$	$3.5193 \cdot 10^{-3}$	$3.6399 \cdot 10^{-3}$	<b><math>3.0036 \cdot 10^{-3}</math></b>	$4.0285 \cdot 10^{-3}$	$3.1937 \cdot 10^{-3}$
312	$6.6208 \cdot 10^{-3}$	$3.0056 \cdot 10^{-3}$	$4.5341 \cdot 10^{-3}$	$3.0455 \cdot 10^{-3}$	$3.2838 \cdot 10^{-3}$	<b><math>2.6363 \cdot 10^{-3}</math></b>	$3.6855 \cdot 10^{-3}$	$2.8286 \cdot 10^{-3}$
624	$6.6386 \cdot 10^{-3}$	$1.7831 \cdot 10^{-3}$	$3.8749 \cdot 10^{-3}$	$1.8214 \cdot 10^{-3}$	$2.0782 \cdot 10^{-3}$	<b><math>1.5614 \cdot 10^{-3}</math></b>	$2.4086 \cdot 10^{-3}$	$1.6609 \cdot 10^{-3}$
1248	$6.6563 \cdot 10^{-3}$	$1.0228 \cdot 10^{-3}$	$3.4142 \cdot 10^{-3}$	$1.0464 \cdot 10^{-3}$	$1.2336 \cdot 10^{-3}$	<b><math>8.7747 \cdot 10^{-4}</math></b>	$1.5129 \cdot 10^{-3}$	$9.5448 \cdot 10^{-4}$

Table 5: The EMSEs of reconstruction from the noisy samples of  $f$  by different methods. The standard deviation of the noise is  $\sigma_\epsilon = 0.05$ . The parameters of  $l_1$  regularization and  $l_2$  regularization are  $\eta = 1.2, \alpha = 1$ .

No. of $S$	MCI	MCI+ Post-filt	$l_1$ -Reg	$l_1$ -Reg+ Post-filt	$l_2$ -Reg	$l_2$ -Reg+ Post-filt
12	$1.5859 \cdot 10^{-1}$	<b><math>1.5599 \cdot 10^{-1}</math></b>	$1.5764 \cdot 10^{-1}$	$1.5764 \cdot 10^{-1}$	$1.5769 \cdot 10^{-1}$	$1.5769 \cdot 10^{-1}$
24	$7.7599 \cdot 10^{-2}$	$7.6884 \cdot 10^{-2}$	$7.7133 \cdot 10^{-2}$	$7.7133 \cdot 10^{-2}$	<b><math>7.6421 \cdot 10^{-2}</math></b>	$7.6421 \cdot 10^{-2}$
36	$1.9784 \cdot 10^{-2}$	$1.8561 \cdot 10^{-2}$	$1.9135 \cdot 10^{-2}$	$1.9135 \cdot 10^{-2}$	<b><math>1.7941 \cdot 10^{-2}</math></b>	$1.7941 \cdot 10^{-2}$
48	$5.4554 \cdot 10^{-3}$	$4.9155 \cdot 10^{-3}$	$5.1145 \cdot 10^{-3}$	$5.1145 \cdot 10^{-3}$	<b><math>4.6144 \cdot 10^{-3}</math></b>	$4.6144 \cdot 10^{-3}$
60	$2.9055 \cdot 10^{-3}$	$2.6568 \cdot 10^{-3}$	$2.7004 \cdot 10^{-3}$	$2.7004 \cdot 10^{-3}$	<b><math>2.5800 \cdot 10^{-3}</math></b>	$2.5800 \cdot 10^{-3}$
72	$2.5378 \cdot 10^{-3}$	$2.3512 \cdot 10^{-3}$	$2.3321 \cdot 10^{-3}$	$2.3321 \cdot 10^{-3}$	<b><math>2.2939 \cdot 10^{-3}</math></b>	$2.2939 \cdot 10^{-3}$
84	$2.4940 \cdot 10^{-3}$	$2.0559 \cdot 10^{-3}$	$2.2026 \cdot 10^{-3}$	$2.0182 \cdot 10^{-3}$	$2.2221 \cdot 10^{-3}$	<b><math>2.0032 \cdot 10^{-3}</math></b>
96	$2.4895 \cdot 10^{-3}$	$1.8232 \cdot 10^{-3}$	$2.1195 \cdot 10^{-3}$	$1.7891 \cdot 10^{-3}$	$2.1736 \cdot 10^{-3}$	<b><math>1.7796 \cdot 10^{-3}</math></b>
108	$2.4909 \cdot 10^{-3}$	$1.6392 \cdot 10^{-3}$	$2.0569 \cdot 10^{-3}$	$1.6031 \cdot 10^{-3}$	$2.1269 \cdot 10^{-3}$	<b><math>1.5973 \cdot 10^{-3}</math></b>
120	$2.4902 \cdot 10^{-3}$	$1.4863 \cdot 10^{-3}$	$1.9990 \cdot 10^{-3}$	$1.4551 \cdot 10^{-3}$	$2.0732 \cdot 10^{-3}$	<b><math>1.4431 \cdot 10^{-3}</math></b>
168	$2.4942 \cdot 10^{-3}$	$1.1034 \cdot 10^{-3}$	$1.8142 \cdot 10^{-3}$	$1.0572 \cdot 10^{-3}$	$1.9003 \cdot 10^{-3}$	<b><math>1.0528 \cdot 10^{-3}</math></b>
216	$2.4956 \cdot 10^{-3}$	$8.8030 \cdot 10^{-4}$	$1.6856 \cdot 10^{-3}$	<b><math>8.3641 \cdot 10^{-4}</math></b>	$1.7557 \cdot 10^{-3}$	$8.3698 \cdot 10^{-4}$
264	$2.4956 \cdot 10^{-3}$	$7.3025 \cdot 10^{-4}$	$1.5669 \cdot 10^{-3}$	<b><math>6.8889 \cdot 10^{-4}</math></b>	$1.6291 \cdot 10^{-3}$	$6.9493 \cdot 10^{-4}$
312	$2.4968 \cdot 10^{-3}$	$6.3040 \cdot 10^{-4}$	$1.4702 \cdot 10^{-3}$	<b><math>5.8854 \cdot 10^{-4}</math></b>	$1.5213 \cdot 10^{-3}$	$5.9541 \cdot 10^{-4}$
624	$2.4994 \cdot 10^{-3}$	$3.3780 \cdot 10^{-4}$	$1.0645 \cdot 10^{-3}$	$3.1709 \cdot 10^{-4}$	$1.0888 \cdot 10^{-3}$	<b><math>3.1546 \cdot 10^{-4}</math></b>
1248	$2.4988 \cdot 10^{-3}$	$1.8447 \cdot 10^{-4}$	$7.0981 \cdot 10^{-4}$	$1.7487 \cdot 10^{-4}$	$7.4399 \cdot 10^{-4}$	<b><math>1.7397 \cdot 10^{-4}</math></b>

Table 6: Comparison of running time (second) on the reconstructions from the noisy samples of  $f$  and  $f'$  by different methods (running 10000 times). The standard deviation of the noise is  $\sigma_\epsilon = 0.1$ . The parameters of  $l_1$  regularization and  $l_2$  regularization are  $\eta = 1.2, \alpha = 1$ .

No. of $S$	MCI	MCI+ Post-filt	Pre-filt +MCI	Pre-filt +MCI+ Post-filt	$l_1$ -Reg	$l_1$ -Reg+ Post-filt	$l_2$ -Reg	$l_2$ -Reg+ Post-filt
12	$3.6788 \cdot 10^0$	$4.3653 \cdot 10^0$	$6.4205 \cdot 10^0$	$8.2292 \cdot 10^0$	$1.1015 \cdot 10^1$	$1.0952 \cdot 10^1$	$3.8853 \cdot 10^0$	$4.1064 \cdot 10^0$
24	$3.8765 \cdot 10^0$	$5.1819 \cdot 10^0$	$7.1325 \cdot 10^0$	$8.6309 \cdot 10^0$	$2.1278 \cdot 10^1$	$2.1175 \cdot 10^1$	$4.4323 \cdot 10^0$	$4.6031 \cdot 10^0$
36	$3.8860 \cdot 10^0$	$6.8050 \cdot 10^0$	$7.8395 \cdot 10^0$	$1.1033 \cdot 10^1$	$4.0122 \cdot 10^1$	$3.9912 \cdot 10^1$	$4.7568 \cdot 10^0$	$4.8133 \cdot 10^0$
48	$4.1999 \cdot 10^0$	$8.4191 \cdot 10^0$	$1.0369 \cdot 10^1$	$1.5357 \cdot 10^1$	$7.4549 \cdot 10^1$	$7.3722 \cdot 10^1$	$5.3805 \cdot 10^0$	$5.4777 \cdot 10^0$
60	$4.1374 \cdot 10^0$	$1.0196 \cdot 10^1$	$1.2337 \cdot 10^1$	$1.8147 \cdot 10^1$	$1.1683 \cdot 10^2$	$1.1920 \cdot 10^2$	$6.4216 \cdot 10^0$	$6.0145 \cdot 10^0$
72	$3.9930 \cdot 10^0$	$1.2222 \cdot 10^1$	$1.4093 \cdot 10^1$	$2.1907 \cdot 10^1$	$1.6636 \cdot 10^2$	$1.6958 \cdot 10^2$	$7.2450 \cdot 10^0$	$7.5104 \cdot 10^0$
84	$4.0059 \cdot 10^0$	$1.4067 \cdot 10^1$	$1.5117 \cdot 10^1$	$2.4300 \cdot 10^1$	$2.1869 \cdot 10^2$	$2.2381 \cdot 10^2$	$7.7516 \cdot 10^0$	$8.2238 \cdot 10^0$
96	$3.9740 \cdot 10^0$	$1.4904 \cdot 10^1$	$1.9453 \cdot 10^1$	$3.0636 \cdot 10^1$	$2.7540 \cdot 10^2$	$2.8930 \cdot 10^2$	$8.8913 \cdot 10^0$	$9.4150 \cdot 10^0$
108	$4.0361 \cdot 10^0$	$1.7351 \cdot 10^1$	$2.1317 \cdot 10^1$	$3.4991 \cdot 10^1$	$3.2556 \cdot 10^2$	$3.3321 \cdot 10^2$	$1.0162 \cdot 10^1$	$1.0759 \cdot 10^1$
120	$4.0246 \cdot 10^0$	$1.8552 \cdot 10^1$	$2.3392 \cdot 10^1$	$3.8498 \cdot 10^1$	$3.7987 \cdot 10^2$	$3.9022 \cdot 10^2$	$1.2139 \cdot 10^1$	$1.2272 \cdot 10^1$
168	$4.1341 \cdot 10^0$	$1.9241 \cdot 10^1$	$3.6574 \cdot 10^1$	$5.3410 \cdot 10^1$	$6.7238 \cdot 10^2$	$6.9768 \cdot 10^2$	$1.7152 \cdot 10^1$	$1.8839 \cdot 10^1$
216	$4.3097 \cdot 10^0$	$2.0494 \cdot 10^1$	$5.9186 \cdot 10^1$	$7.8245 \cdot 10^1$	$1.1883 \cdot 10^3$	$1.2520 \cdot 10^3$	$4.1561 \cdot 10^1$	$4.2246 \cdot 10^1$
264	$5.3899 \cdot 10^0$	$2.5877 \cdot 10^1$	$9.8980 \cdot 10^1$	$1.1487 \cdot 10^2$	$1.8915 \cdot 10^3$	$1.9623 \cdot 10^3$	$6.6949 \cdot 10^1$	$6.9506 \cdot 10^1$
312	$5.4321 \cdot 10^0$	$2.7976 \cdot 10^1$	$1.2620 \cdot 10^2$	$1.4583 \cdot 10^2$	$2.8349 \cdot 10^3$	$2.9861 \cdot 10^3$	$1.1200 \cdot 10^2$	$1.0305 \cdot 10^2$
624	$1.0396 \cdot 10^1$	$4.5142 \cdot 10^1$	$7.1446 \cdot 10^2$	$7.2646 \cdot 10^2$	$1.2915 \cdot 10^4$	$1.2899 \cdot 10^4$	$5.1578 \cdot 10^2$	$5.0876 \cdot 10^2$
1248	$2.3852 \cdot 10^1$	$8.2320 \cdot 10^1$	$3.4522 \cdot 10^3$	$3.5232 \cdot 10^3$	$3.4581 \cdot 10^4$	$3.4218 \cdot 10^4$	$2.9432 \cdot 10^3$	$3.1514 \cdot 10^3$

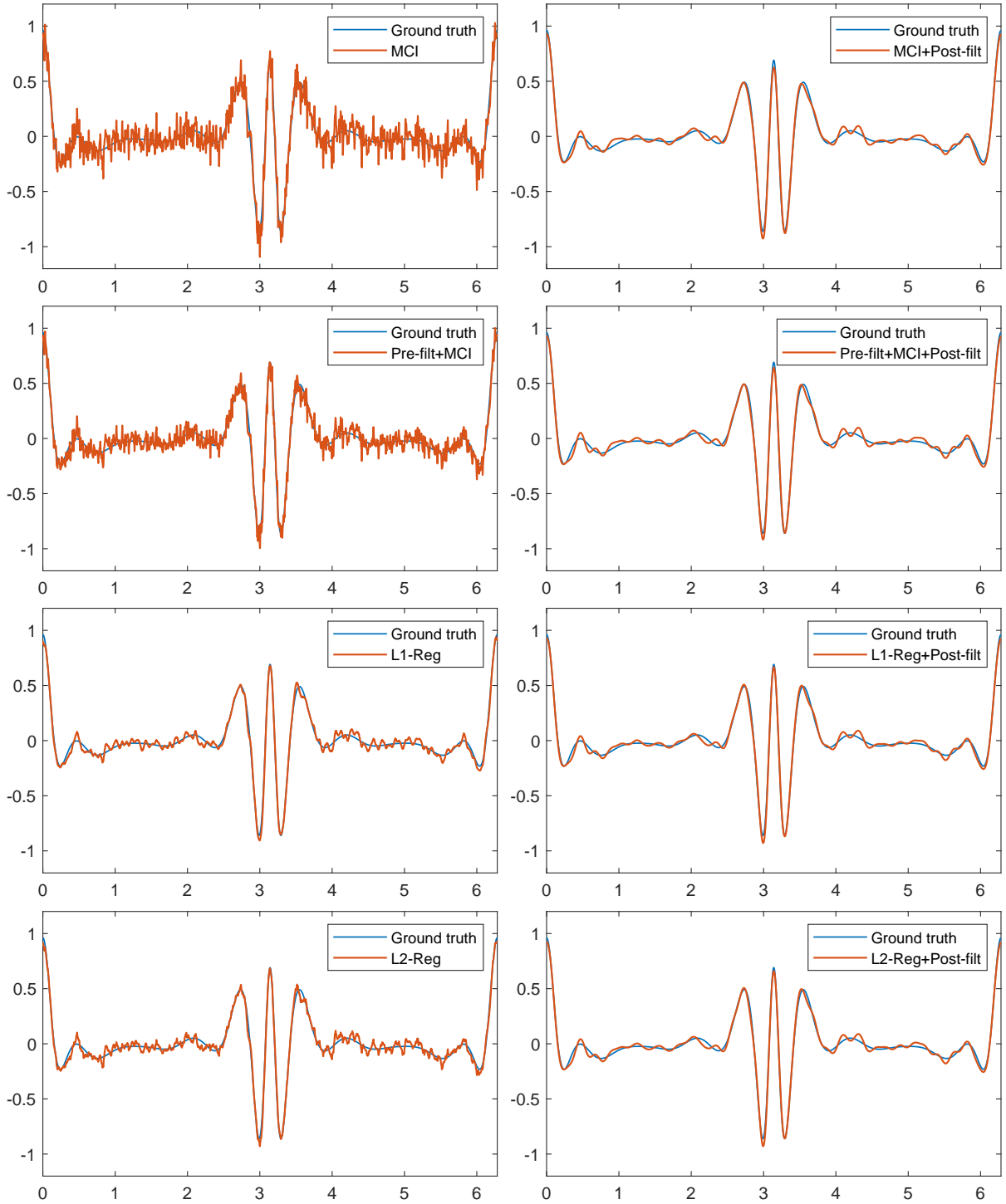


Figure 5: The reconstructed results (red lines) by different methods under the sampling scheme of FD2 in the noisy environment with  $N_s = 1248$ ,  $\sigma_\epsilon = 0.1$ ; the blue line is the original test function  $f(t)$ . The parameters of  $l_1$  and  $l_2$  regularization are  $\eta = 1.2$ ,  $\alpha = 1$ .

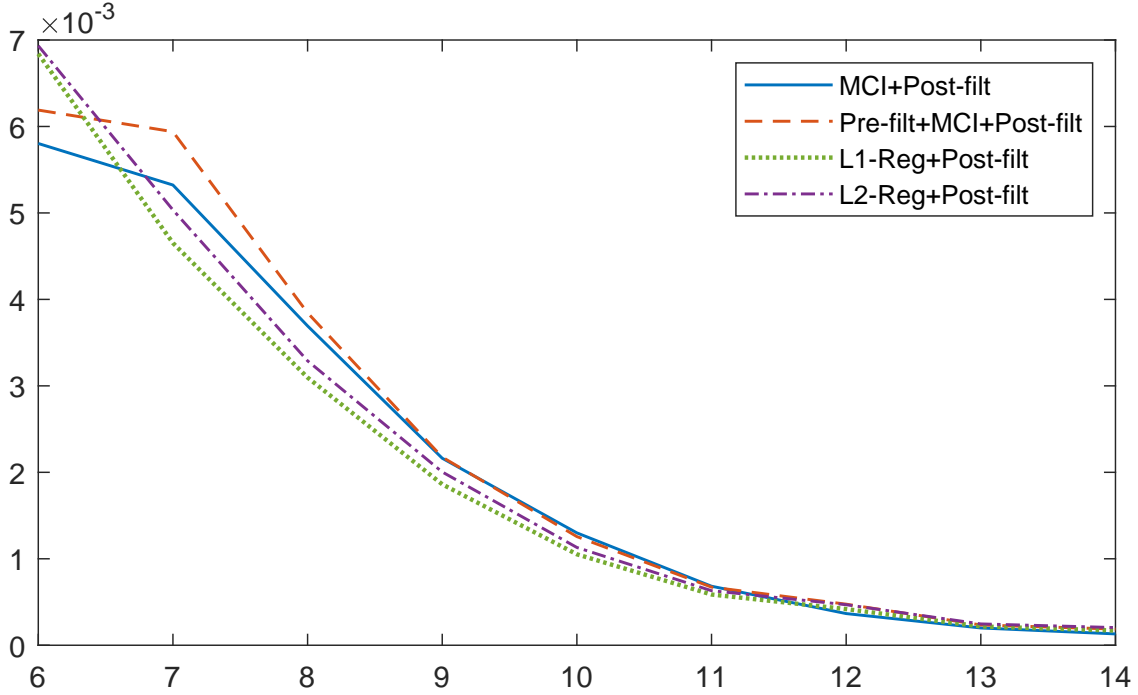


Figure 6: Experimental convergence analysis. The horizontal axis represents  $\log_2 N_s$ , where  $N_s$  is the total number of samples. The vertical axis represents the error of reconstruction.

## References

- [1] A. Papoulis, “Generalized sampling expansion,” *IEEE Trans. Circuits Syst.*, vol. 24, no. 11, pp. 652–654, 1977.
- [2] K. Gröchenig, J. Romero, and J. Stöckler, “Sharp results on sampling with derivatives in shift-invariant spaces and multi-window Gabor frames,” *Constructive Approximation*, vol. 51, no. 1, 2020.
- [3] U. J. Mönich and H. Boche, “A two channel system approximation for bandlimited functions,” *IEEE Transactions on Information Theory*, vol. 63, no. 9, pp. 5496–5505, 2017.
- [4] N. Liu, R. Tao, R. Wang, Y. Deng, N. Li, and S. Zhao, “Signal reconstruction from recurrent samples in fractional Fourier domain and its application in multichannel SAR,” *Signal Processing*, vol. 131, pp. 288–299, 2017.
- [5] L. Xu, R. Tao, and F. Zhang, “Multichannel consistent sampling and reconstruction associated with linear canonical transform,” *IEEE Signal Processing Letters*, vol. 24, no. 5, pp. 658–662, 2017.
- [6] F. A. Shah and A. Y. Tantary, “Lattice-based multi-channel sampling theorem for linear canonical transform,” *Digital Signal Processing*, vol. 117, p. 103168, 2021.

- [7] D. Wei and Y. M. Li, "Convolution and multichannel sampling for the offset linear canonical transform and their applications," *IEEE Trans. Signal Process.*, vol. 67, no. 23, pp. 6009–6024, 2019.
- [8] D. Cheng and K. I. Kou, "Multichannel interpolation of nonuniform samples with application to image recovery," *J. Comput. Appl. Math.*, vol. 367, p. 112502, 2020.
- [9] A. Wigderson and Y. Wigderson, "The uncertainty principle: variations on a theme," *Bulletin of the American Mathematical Society*, vol. 58, no. 2, pp. 225–261, 2021.
- [10] L. Xiao and W. Sun, "Sampling theorems for signals periodic in the linear canonical transform domain," *Opt. Commun.*, vol. 290, pp. 14–18, 2013.
- [11] E. Mohammadi and F. Marvasti, "Sampling and distortion tradeoffs for bandlimited periodic signals," *IEEE Transactions on Information Theory*, vol. 64, no. 3, pp. 1706–1724, 2018.
- [12] D. Cheng and K. I. Kou, "FFT multichannel interpolation and application to image super-resolution," *Signal Process.*, vol. 162, pp. 21 – 34, 2019.
- [13] D. Fraser, "Interpolation by the FFT revisited-an experimental investigation," *IEEE Transactions on Acoustics, Speech, and Signal Processing*, vol. 37, no. 5, pp. 665–675, 1989.
- [14] M. Pawlak, E. Rafajlowicz, and A. Krzyzak, "Postfiltering versus prefiltering for signal recovery from noisy samples," *IEEE Trans. Inf. Theory*, vol. 49, no. 12, pp. 3195–3212, 2003.
- [15] M. Grant and S. Boyd, "CVX: Matlab software for disciplined convex programming, version 2.1," <http://cvxr.com/cvx>, Mar. 2014.
- [16] J. Chen, J. Benesty, Y. Huang, and S. Doclo, "New insights into the noise reduction Wiener filter," *IEEE Trans. Audio Speech Lang. Process.*, vol. 14, no. 4, pp. 1218–1234, 2006.
- [17] S. Ramani, D. Van De Ville, T. Blu, and M. Unser, "Nonideal sampling and regularization theory," *IEEE Trans. Signal Process.*, vol. 56, no. 3, pp. 1055–1070, March 2008.
- [18] D. Donoho, M. Elad, and V. Temlyakov, "Stable recovery of sparse overcomplete representations in the presence of noise," *IEEE Transactions on Information Theory*, vol. 52, no. 1, pp. 6–18, 2006.
- [19] H. Ohlsson, L. Ljung, and S. Boyd, "Segmentation of ARX-models using sum-of-norms regularization," *Automatica*, vol. 46, no. 6, pp. 1107–1111, 2010.
- [20] S. Boyd, N. Parikh, E. Chu, B. Peleato, and J. Eckstein, "Distributed optimization and statistical learning via the alternating direction method of multipliers," *Foundations and Trends® in Machine Learning*, vol. 3, no. 1, pp. 1–122, 2011.
- [21] C. Zou and K. I. Kou, "Robust signal recovery using the prolate spherical wave functions and maximum correntropy criterion," *Mech. Syst. Signal Proc.*, vol. 104, pp. 279–289, 2018.